

Lateral Variation of P Velocity in The Himalayan Crust
and Upper Mantle

a study based on observations of teleseisms at the
Tarbela Seismic Array

by

William Henry Menke

S.B., Massachusetts Institute of Technology

1976

Submitted in Partial Fulfillment of the
Requirements for the Degree of
Master of Science

at the

Massachusetts Institute of Technology

May, 1976

Signature of Author ^{05/03/76}
Department of ~~Earth and Planetary Science~~

Certified by
Thesis Supervisor

Accepted by
Chairman, Departmental Committee

Lindgren
~~WITHDRAWN~~
JUL FROM 1976
MIT LIBRARIES

Contents

Abstract	1
Introduction	3
Discussion of Data	7
Calculation of Travel Time Residuals	13
Preliminary Examination of Data	18
Inversion of the Data	24
Implication to Geologic Structure	44
Conclusions	49
Appendix One	50
Appendix Two	61
Acknowledgements	71
Bibliography	72

Abstract

Three dimensional geologic structures within the earth give rise to P velocity distributions that depart significantly from the simplistic plane layered models often used by seismologists to describe them. These Three dimensional velocity distributions are observable even they occur to depths of several hundred kilometers, and can be reconstructed by inverting earthquake first arrival data. From this reconstructed velocity distribution an understanding of the nature of the geologic structures can be obtained, especially if other geologic and geophysical constraints are available.

A simple type of such an inversion developed by K. Aki, et al(1975) is used in this study to observe geologic structure in the vicinity of the Tarbela seismic array in northern Pakistan to a depth of 125 kilometers. Since this array is located at the western extreme of the Main Boundary Fault of the southwestern Himalayas, constraints on the tectonics of the Indian-Eurasian plate collision are obtained.

Travel time residuals from 122 teleseisms are inverted to estimate velocity perturbations above and below an initial plane layered model of the Tarbela array. The main features of this inversion are a clear elongation of velocity anomalies in the northwest direction and a general 2 to 3 percent decrease in velocity across any horizontal

layer to the northeast. These features are interpreted as a 4 degree dip of geologic structures in the direction $N41^{\circ}E$. This direction is compatible with trends of seismicity in the Tarbela area and with the trend of the Main Boundary Thrust southeast of Tarbela, but not with the trend of the fault trace nor the strike of geologic structure in the Tarbela area. Locally the faults bend sharply westward after a loop called the Hazara Syntaxis. The author concludes that the westerly trending surface fault trace and westerly striking geology are both superficial and not representative of structures at greater depth. These deep structures within the crust and upper mantle preserve a strike similar to more eastern areas along the Main Boundary Thrust. They are shown to be volumetricly and tectonicly the more important features.

Introduction

The Himalayan mountains constitute an important part of the collision zone between the Indian and Eurasian plates (see Figure 1). However because of their physical inaccessibility, and other political and economic factors, detailed geophysical data for this region are scarce. Features observable on the surface or on satellite photographs, such as outcropping stratigraphic units, fault traces and relief, can be used to the very large scale (10^3 to 10^4 kilometers) structural and dynamical features of this region. This has been shown, for instance, by Molnar and Tapponnier (1975). However, even with the most avid extrapolation, surface features elucidate the medium scale (10^2 kilometers) structure of only the first few kilometers of crust. In contrast, plate tectonics suggests that dynamically evolving structures exist to depths perhaps fifty times as great. To understand the details of the structure of these plates, in the region severely influenced by their collision, requires reliance on this *scarce* geophysical data.

Present sources of such data are limited to gravity measurements, seismicity maps, refraction and surface wave dispersion studies using nearby WWSSN seismic stations, and similar seismic data from local short period instruments. Gravity data do not extend throughout the entire Himalayan range. They are limited to the southwestern half of a range

that has a general northwest strike. Unfortunately it is in this *unsampled* region that major differences between several hypothetical plate geometries appear, as was noticed by Warsi (1976).

A lack of available seismic stations to the north of the Himalayas makes hypocenter location and depth resolution poor. Refraction and dispersion studies suffer from the averaging effects of waves passing across the strike of geologic structures from hypocenters in the Himalayas or to their north to seismic stations located in the Indian shield.

The bulk of short period data, for the western Himalayas at least, comes from the Tarbela seismic array. This array is located around the Tarbela damsite in northern Pakistan, and is maintained by the Lamont-Doherty Geological Observatory of Columbia University. The array site is a few kilometers south of the Hazara Syntaxis, a loop in the Himalayan Main Boundary Thrust (see map of array in figure 10). Since this region is seismically active it has been possible to produce three dimensional seismicity maps and composite fault plane solutions for selected areas in the array vicinity. Since the array also records teleseisms it is possible to observe changes imposed on the ray parameter vector (*ie.* azimuth, ray parameter) and patterns of travel time residuals caused by structures at depth, in order to learn the nature of these structures.

The process and results of an investigation of local array structure consisting of an examination of teleseismic data will be described below. Constraints on the dip of the Moho in this region are discussed. Lateral variations in P velocity are *determined up* to a depth of 125 kilometers by an inversion technique recently developed by K.Aki, et al. (1975). While no strong claim can be made that these structures are typical of the Himalayas in general, or even other parts of the Main Boundary Thrust, a knowledge of the deep structure of the Syntaxis will help constrain models of the tectonics of the western Himalayas as a whole.

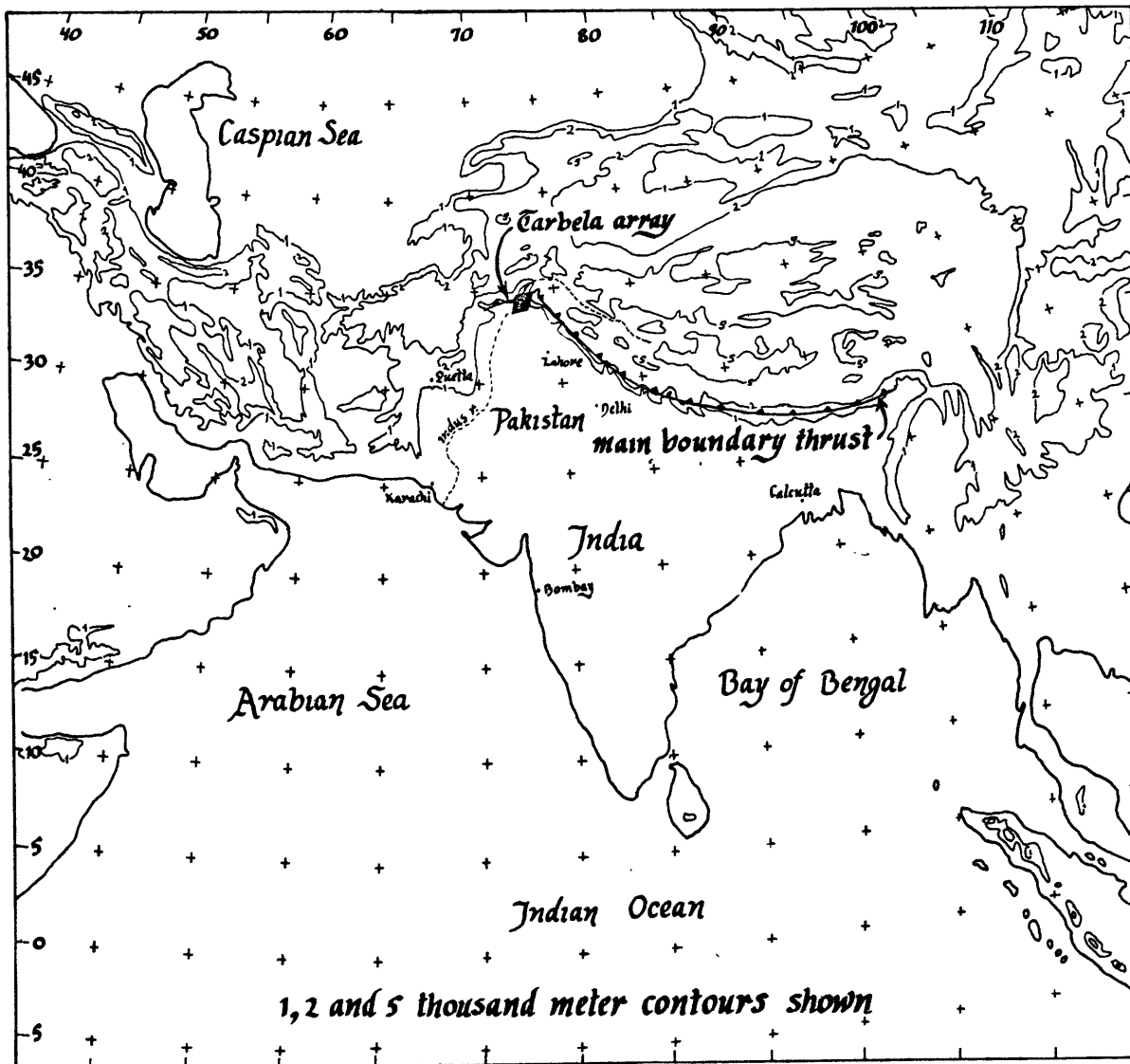


Figure 1 : Map of India and Pakistan showing elevation contours and some political features. The Tarbela array, from which this study is based, is the diamond shaped marking in the southwestern Himalayas, at the western extreme of the Main Boundary Thrust. The 'Z' shaped ridge near Quetta is the Baluchistan Arc.

Discussion of Data

The data used in this investigation consist of arrival times from 122 teleseisms, from a wide range of distances and azimuths, recorded by at least five of the stations of the Tarbela array. The average number of stations recording any one event was about 8. The final data set consisted of slightly over 1000 arrival times. These data were collected by the author by examining the original Teledyne Geotech Develocorder traces, using Preliminary Determination of Epicenter (P.D.E.) monthly listings as a guide to when potentially useful events occurred. Photocopies of these events were made and referred to at various times during the data reduction process. While the Tarbela array has been operating for approximately three years, local noise levels prevent records from about one third that time from providing useful teleseismic data. Nevertheless this period constitutes sufficient time to gather good coverage from eastern azimuths, which include Pacific Benioff zone events. Coverage from northern and western azimuths is somewhat less complete but still adequate. Coverage of southern azimuths is poor. Only a few events from the Indian rise and Africa were recorded. A Mercator plot of epicenters of events used in the study is provided in figure 3.

Arrival times for events, in order to contribute meaningful data to this study, must be measured \longrightarrow
 \longrightarrow within 0.1 second or better.
Since the record of first motion is often not clear on Tar-

bela records, no effort was made to pick it. Rather a reference point at the beginning of the P wave train, usually a large peak or trough, was identified and measured at each station. This was accomplished by either visually selecting what appeared to be the appropriate peak, or in more obscure cases by matching peaks by means of traced templates.

Some information about the local velocity structure is lost when the first motions are not picked. In particular the vertical velocity gradient can no longer be resolved. This can be understood by picturing a teleseismic wavefront moving up through the lithosphere (see figure 2a), starting as a plane wave at the bottom, but becoming increasingly corrugated as it encounters inhomogeneties at shallower depths. Since the travel time for any point on this wavefront is not measured, no recovery of vertical structure can be made. But the degree of corrugation, which reflects differences in travel time across the array, is measured. While net, or absolute travel time residuals can not be determined, these relative residuals can be. Two different methods for determining these residuals will be discussed below.

Arrival data were cleaned by several methods to improve their internal consistency. While it is possible that such a process may introduce bias into the data, uncleaned data was found to contain too much noise to produce interpretable results. In this sense cleaning was considered nec-

essary.

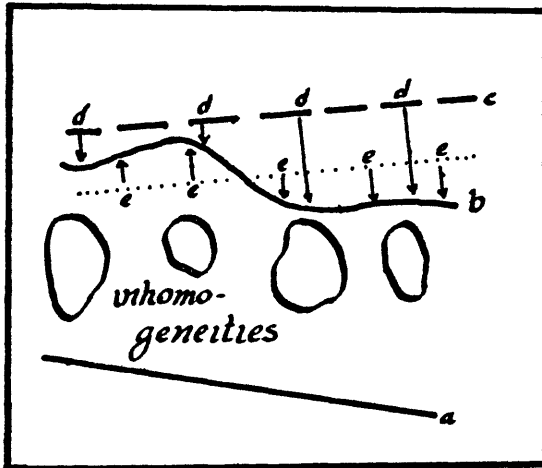
The first step in the cleaning process was to fit, by the method of least squares, a plane wave to the arrival data. Ray parameter vector data from this regression analysis were compared to theoretical calculations to confirm that each event was properly identified. Residuals relative to the plane wave were then inspected. Where they exceeded 0.5 second they were suspected of being caused by picking a reference point one cycles off from the correct one on the original seismogram (a typical teleseismic cycle is 0.75 second). Records for these events were double checked and corrected where it seemed advisable.

Relative travel time residuals for all events were then plotted, station by station, against azimuth. Of course, since these residuals are being ascribed to three dimensional velocity variations beneath the array, they are expected to be a function of angle of incidence also. Later stages of analysis consider them to be such. However, since most of the data has an angle of incidence between 20 and 30 degrees, the azimuthal dependence is taken to be the stronger of the two. Scatter around a general trend represents either errors in measuring arrival times or raypaths of unusual angle of incidence. The last part of the cleaning process consisted of examining each point that fell far from the general trend in the azimuth vs. residual plot, ascribing the scatter to one of these two causes, and re-

moving it in the case of the former.

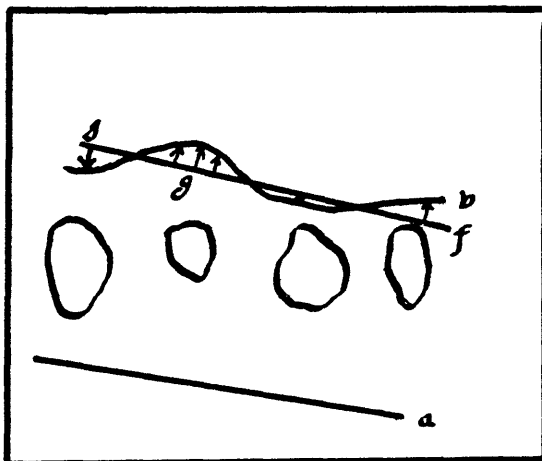
The final result was a data set of arrivals from 122 teleseismic events that displayed a high degree of internal consistency.

figure 2 methods of calculating travel time residuals



a. p.d.e.-j.b. method

- a. wavefront at time = t_1
- b. wavefront at time = t_2
- c. wavefront as predicted by standard earth model at t_2
- d. distances on which absolute travel time residuals are based
- e. distances on which relative residuals are based



b. plane wave method

- f. best fitting plane wave
- g. relative travel time residuals

note that if the velocity structure changes the average ray parameter, methods a. and b. give different results.

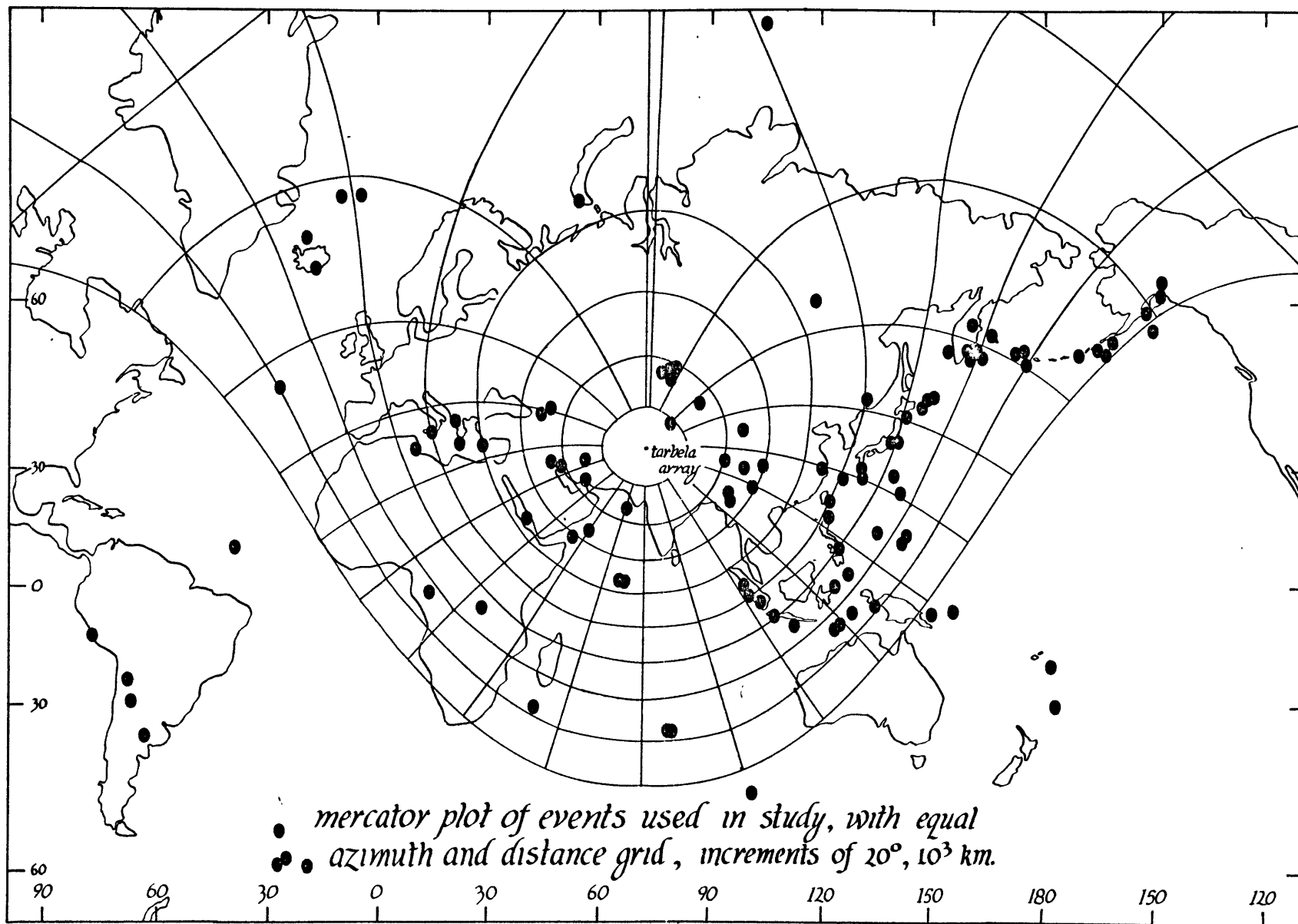


Figure 3 : Map showing distribution of events used in study.

Calculation of Travel Time Residuals

Travel time residuals have been computed from the arrival data by two methods which in general produce different results. The first, herein called the Preliminary Determination of Epicenter - Jefferys-Bullen (P.D.E.-J.B.) method, consists of calculating theoretical arrival times for each event, using the P.D.E. hypocenter locations and origin times, the J.B. travel time curves for P and PKP phases, and elliptical earth geometry. These arrival times were then subtracted from the observed arrival times to produce residuals. Since first motions are not picked, the residuals are generally found to be negative and several seconds in magnitude. The mean residual is then subtracted from the residuals for each event to produce a set of relative residuals that reflect the corrugation of the wavefront. The ray parameter vector calculated by the P.D.E.-J.B. method need not coincide with the vector as measured at the array site (by fitting a plane wave to the arrival data), If the difference, or residual ray parameter, is attributable to velocity gradients within the Tarbela array, then this method provides useful information about those gradients. If however they are due to source effects, or to errors in computing the ray parameter from the travel time tables, then they bias any reconstruction of the local velocity structure.

The second method avoids problems associated with us-

ing standard locations and travel times by, in effect, using the arrival data to calculate these quantities. The ray parameter vector is determined by fitting a plane wave to the data by a linear regression. Residuals are measured relative to this plane wave, and already have zero mean. By this method no errors can be introduced by either source effects or regional propagation effects, as long as these do not corrugate the plane wave. Unfortunately the average velocity gradient across the array may no longer be resolved. Structures that shift a plane wave uniformly, such as a dipping interface, are not seen by this method. In contrast the P.D.E.-J.B. method would detect them. Relative residuals are plotted against azimuth in Figure 4. The smaller magnitude of the residuals calculated by the plane wave method is a result of losing two degrees of freedom from the arrival data when determining the components of the ray parameter vector. Both methods of calculating residuals are presented schematically in Figure 2.

Relative Travel Time Residuals —

p.d.e. - j.b. plane wave

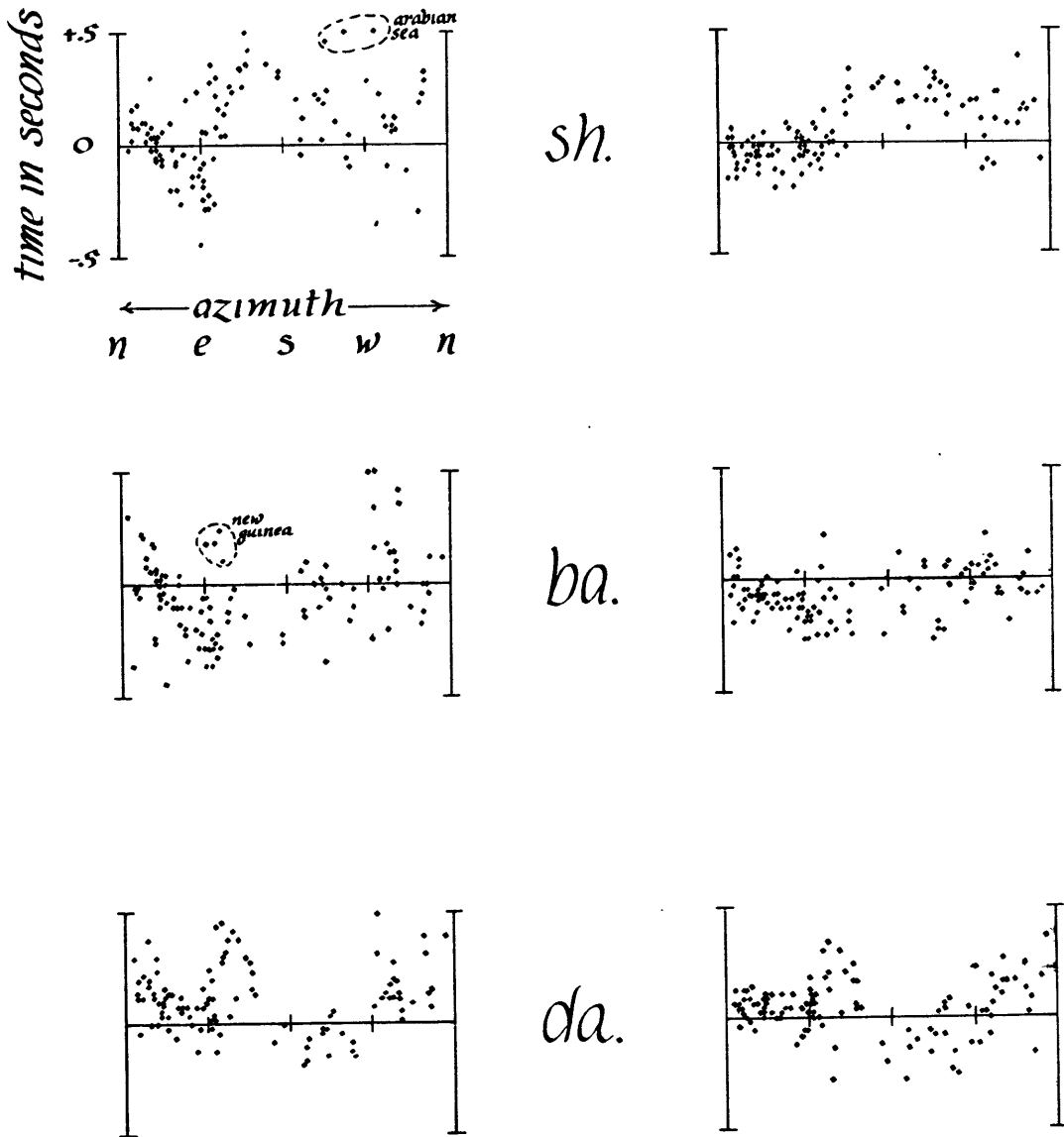


Figure 4 : Relative travel time residuals plotted against azimuth for each station of the Tarbela array. To the left of each station abbreviation (sh, ba, qi, etc.) data is presented using the "P.D.E.-J.B." method of calculating residuals. To the right of each abbreviation is the same data, processed by the "plane wave" method.

Relative Travel Time Residuals continued
 p.d.e. - j.b. plane wave

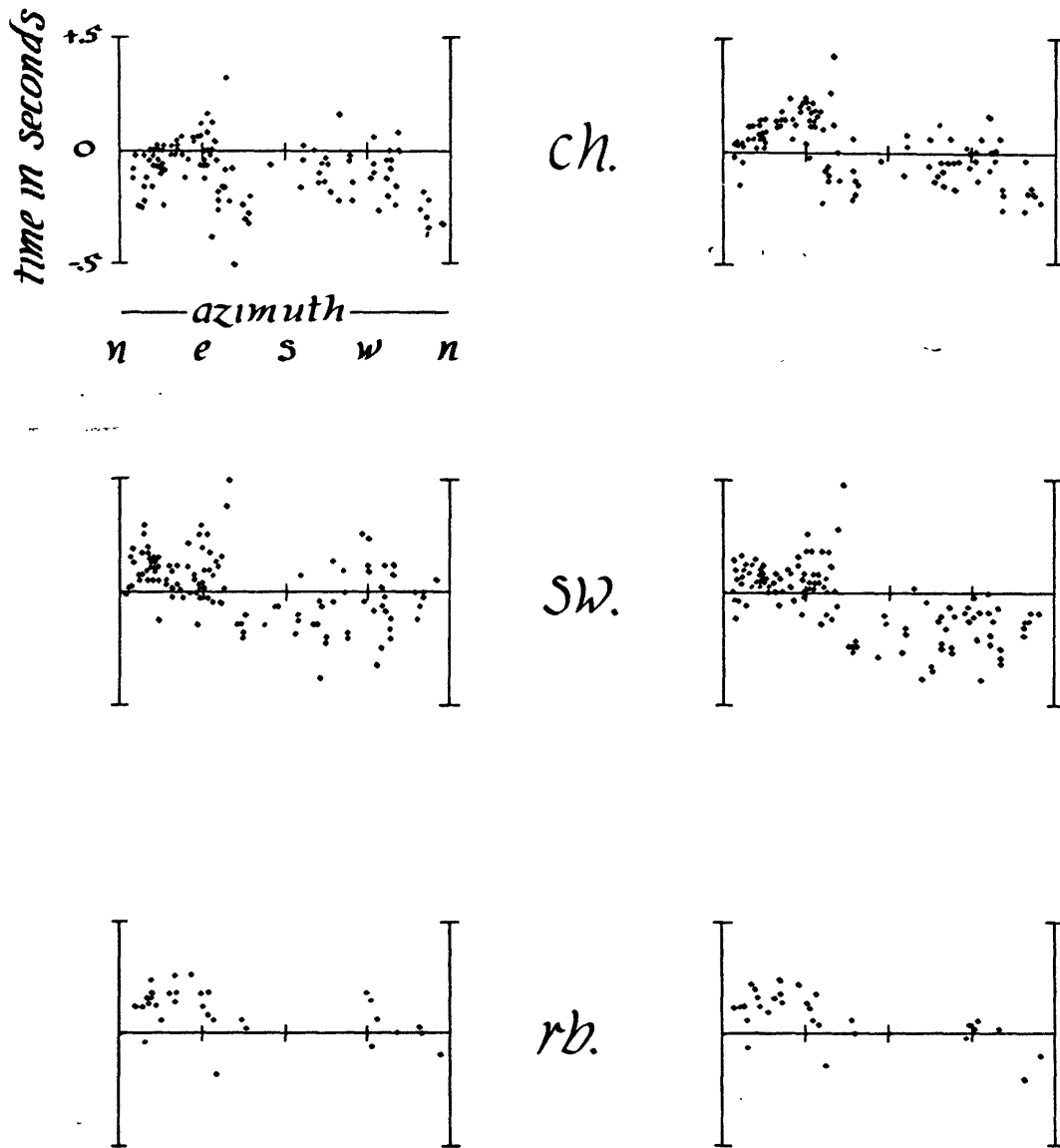


Figure 4 (con't)

Relative Travel Time Residuals continued
 p.d.e. -j.b. plane wave

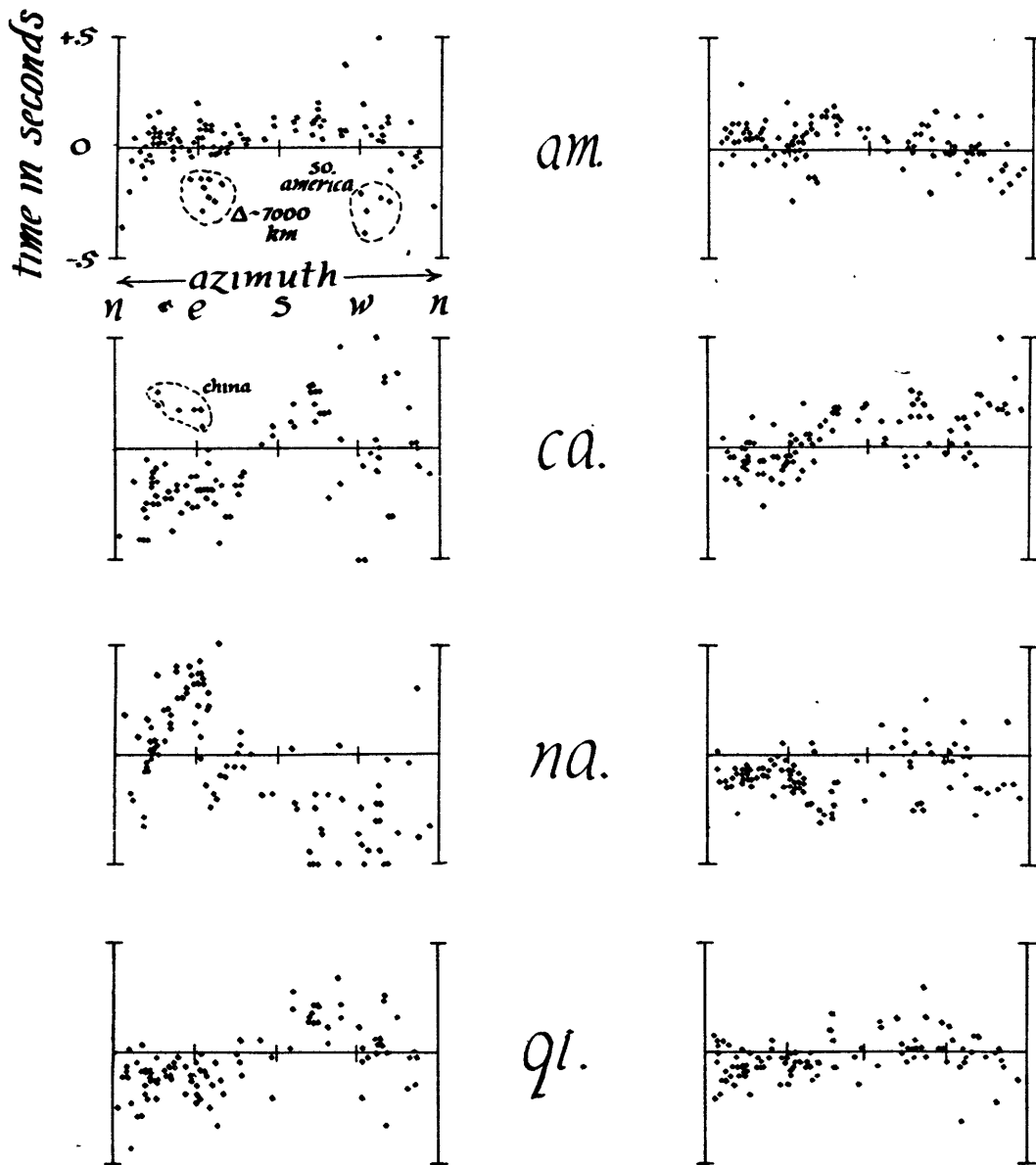


Figure 4 (con't).

Preliminary Examination of Data

The ray parameter vector information obtained through the linear regression can be used to examine gross changes imposed on the ray parameter vector by structures under the array. Such a method uses no complicated inversion techniques, but rather consists of comparing, in some graphical manner, the ray parameter vector for each event as observed by the linear regression and as predicted by the F.D.E.-J.B. method. Such a comparison is shown in Figure 5.

Any interpretation of Figure 5 must involve a careful consideration of factors which may influence measurement of the ray parameter vector. Since the Tarbela array is not located on a horizontal surface, but rather rests on terrain whose elevation increases northeastward, elevation effects must be removed from the arrival data in order to correctly determine the ray parameter vector. This in turn requires a knowledge of the P velocity in the top kilometer of the array, which in fact has not been determined in any exact sense. Secondly the actual depth of the velocity gradients responsible for changing the ray parameter vector can not be determined. While the author shall argue that they are local, resulting from a dipping Moho, one could equally well argue, on the basis of these data alone, that much shallower or deeper gradients, or even source effects (as is argued by Davies and Sheppard (1972) in connection with the LASA array) contribute significantly to the observed shifts.

A crude idea of the near surface P velocity can be obtained by examining the variation of the mean residual for all events measured at one station as a function of the elevation of that station. Although many factors, including shallow inhomogeneties that effect only one station, may contribute to the mean residual, elevation may reasonably be expected to dominate the effect. A plot of mean station residual vs. station elevation is shown in Figure 7. Considerable scatter is present, but r relatively high stations tend to be relatively late. \longrightarrow This variation is more or less consistant with a velocity of 5 km/sec in the upper kilometer of the crust. Certainly this is a simplification since the velocity under each station may vary from station to station. Never the less the effects of a 5 km/sec layer has been removed from the arrival data.

Upon examining the array diagram in Figure 5, a consistant shift in the ray parameter is discovered. In particular the ray parameter is shifted about 0.36 ± 0.05 sec/deg in the direction $N232^{\circ}E_{+1}^{\circ}$. As shown in Figure 6, such a shift can result from a dipping interface, and is approximately independent of the ray parameter vector of each event. The author shall assume that this dipping interface represents the Moho. Such an assumption is justifiable on the grounds that in general the largest velocity contrasts are to be found at the Moho. It is also justifiable on the grounds that a Moho dipping, as the data

suggest, in the northeastern direction is compatible with several recent tectonic models of the Himalayas which consider portions of the Indian Plate thrusting under the material to the northwest. If the Moho velocity contrast is assumed to be 6.4 to 7.8 km/sec, the observed shift in the ray parameter corresponds to a dip of about 7 degrees.

Since no elevation corrections have been made to these data, and since the slope of topography produce a shift in the same direction as the dipping interface, a dip of 7 degrees should be considered a maximum dip. When the data are corrected for elevation, the shift in the ray parameter is smaller : 0.20 ± 0.05 sec/deg in the direction $N221^{\circ}E \pm 1^{\circ}$. This corrected shift leads to a best estimate of Moho dip of 4 degrees in the direction $N41^{\circ}E$. Since the choice of a near surface velocity of 5 km/sec may have either over- or undercompensated for the effect of station elevation, this estimate should be viewed as having an uncertainty of 2 or 3 degrees. Regardless of the actual magnitude of the dip, a dip in the northeastern direction is compatible with the trend of the Main Boundary Fault southeast of Tarbela, and with the trend of the zone of high seismicity that occurs just to the north of the array (see Figure 10).

Array Diagrams - no elevation corrections

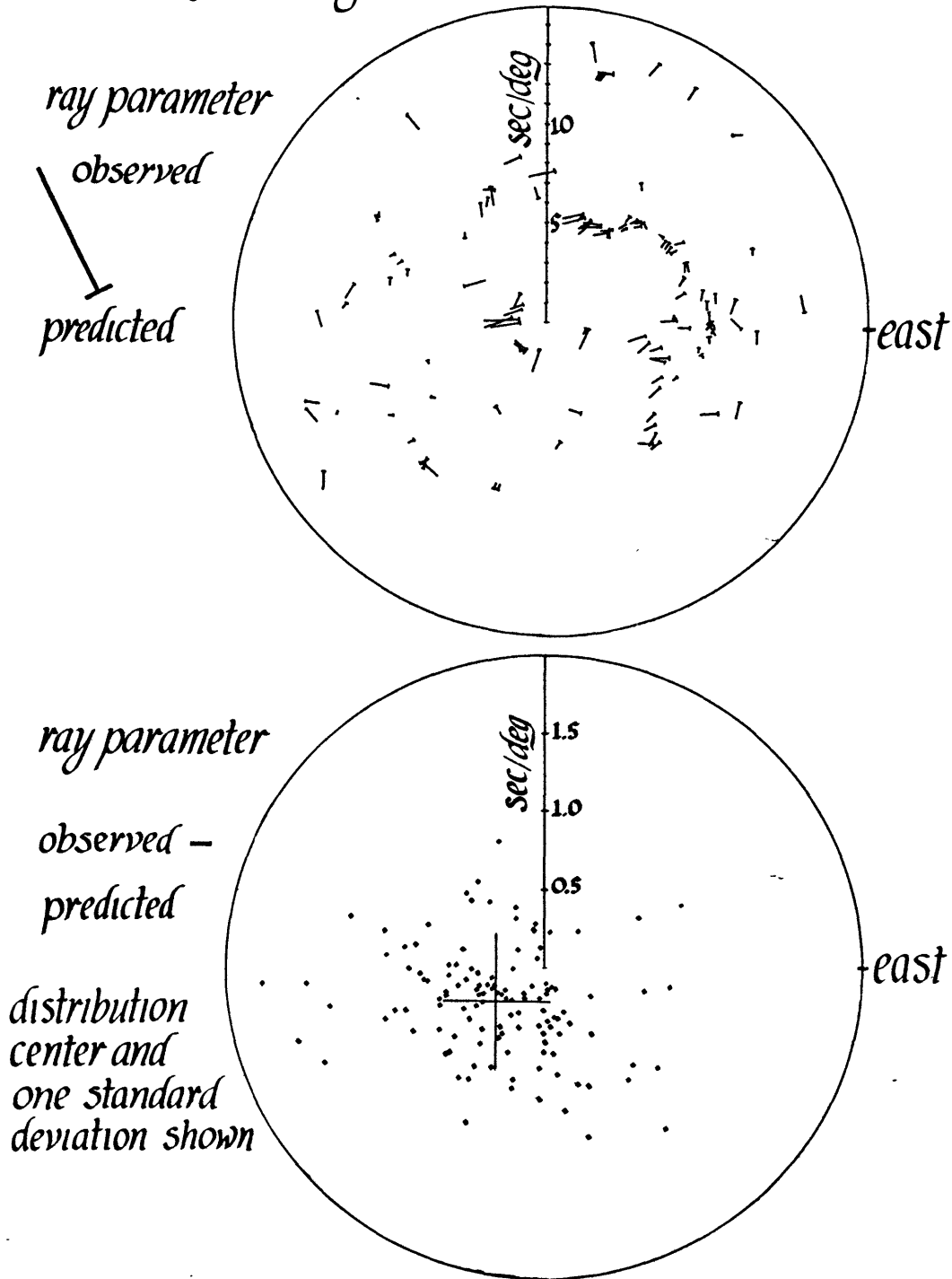
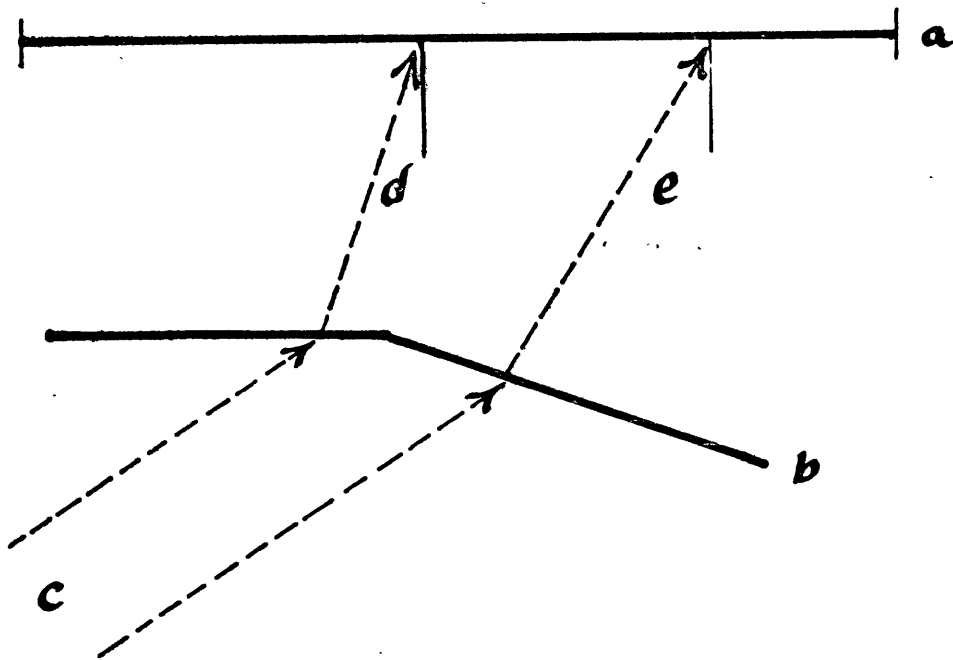


Figure 5 : Ray parameter residuals plotted against azimuth and ray parameter. Note the average shift of the vectors to the southwest, compatible with a Moho dipping to the northeast at 7 degrees.

modification of ray parameter by dipping interface



- a. surface of earth
- b. interface horizontal to left, dipping to right
- c. parallel seismic rays
- d. angle of incidence of ray passing through horizontal interface
- e. same for dipping interface. note $d \neq e$.

Figure 6 : The ray parameter of a teleseism, as measured by a seismic array, can be altered if a dipping interface exists below the array.

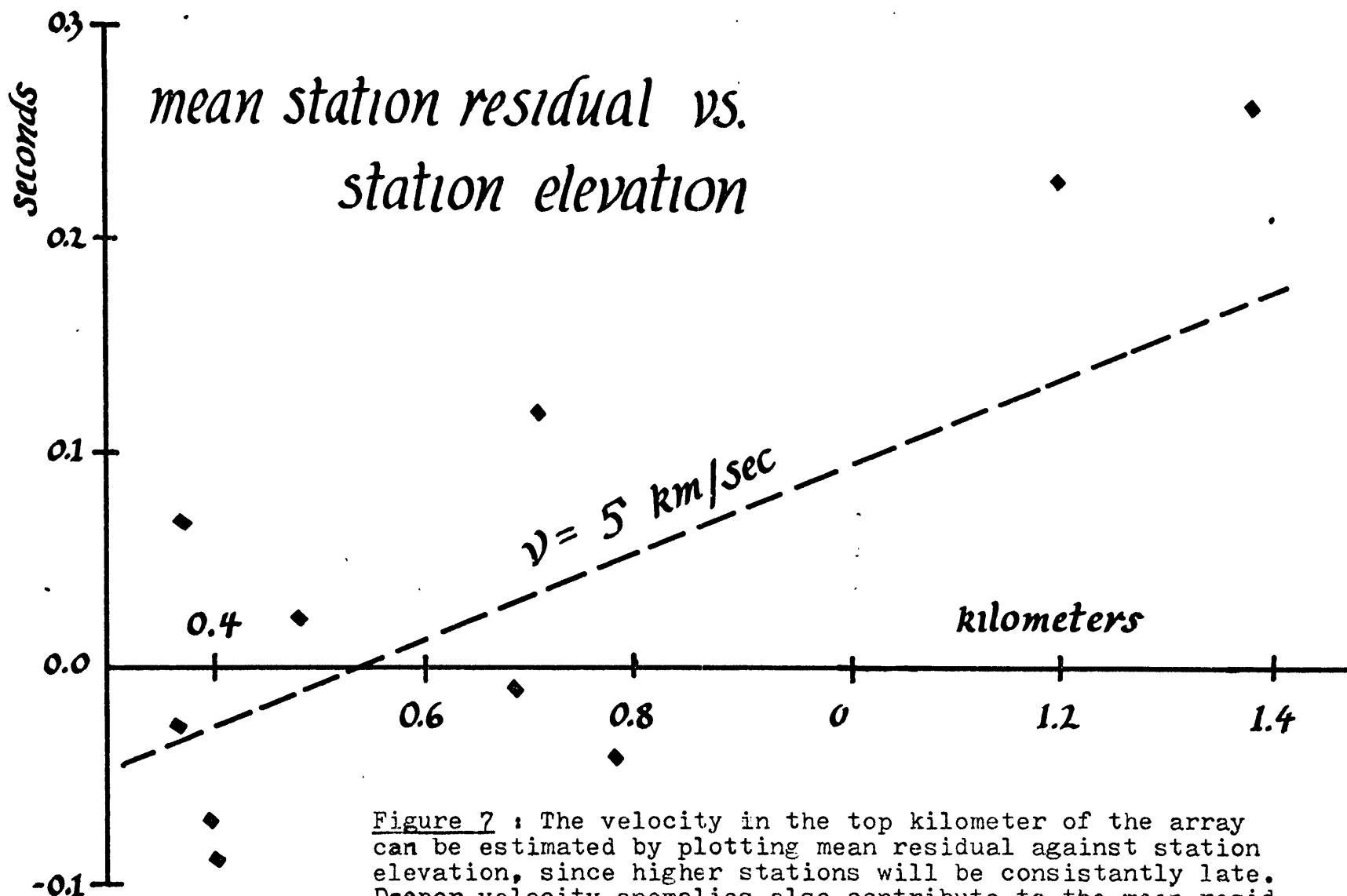


Figure 7 : The velocity in the top kilometer of the array can be estimated by plotting mean residual against station elevation, since higher stations will be consistently late. Deeper velocity anomalies also contribute to the mean residual of a station, adding scatter to the plot. The observed trend is compatible with a 5 km/sec P velocity immediately under the array.

Inversion of the Data

The travel time residuals shown above have been inverted by the method of K. Aki, et al (1976). Solutions to the matrix equations they derive have been found by the damped least squares method of Levenberg (1944). This method provides stable, although somewhat smoothed solutions. The inversion yields a first order estimate of the velocity perturbations necessary to minimize the summed squares of the travel time residuals, when an initial plane layered model has been divided into a number of blocks and the velocity of each block allowed to vary independently. Because relative residuals are used, the velocities in each layer are determined only up to an overall additive constant.

Only small (less than one percent) errors seem to result from using an initial model that departs from the actual laterally average velocity structure by as much as ten percent. It is nevertheless desirable to choose an initial model that is approximately correct for the Tarbela area. For this purpose a set of velocity models for the Himalayas were taken from the literature and compared in Figure 8. This set includes five refraction studies, two of which correspond to the southern Himalayan foothills, and a structure currently used to locate events around the Tarbela array by the Hypo '71 location program.

The Tarbela structure was designed to adequately locate both explosions at the Tarbela damsite and earthquakes of known hypocenter outside the array. Since the Tarbela structure closely resembles the Himalayan foothill models, the former was used as an initial model in the inversion. The crustal layers of this model were averaged into one homogeneous crust, of velocity 6.1 km/sec overlying a mantle of velocity 7.8 km/sec. The Moho is taken to be at a depth of 33 kilometers. Four layers were cut from this initial model and further divided into 280 blocks each 20 x 20 kilometers in width. Velocity perturbations, in percent above and below the average velocity of each layer were determined for as many blocks as data permitted. The uppermost layer in the inversion is taken to represent the crust, the lower three layers the upper 120 kilometers of the mantle. The initial model is specified in Table 1.

The P.D.E.-J.B. and plane wave residuals were used to construct two laterally varying Tarbela velocity structures. These are shown as three dimensional constructions in Figure 9. Only the blocked in area of each layer has been resolved, and within that area low velocity regions have been shaded. Contour maps, correlatable with seismicity and geologic maps have been provided in Figure 10. Each contour corresponds to a one percent perturbation of the original velocity model. It should be noted that the edges of the inversion do not correspond to the north and east

directions in the Tarbela area but are rotated 16 degrees counterclockwise with respect to them.

The two inversions shown in Figure 9 show considerable similarity. Most differences can be accounted for by the different resolving powers of the two methods, and by the difficulty in resolving average lateral gradients by the plane wave method. The crustal layer shows a saddle shaped velocity structure, with low velocity regions in the northeast and southwest quadrants. The maximum contrast occurs in the crustal layer, amounting to somewhat more than 5 percent or 0.3 km/sec, in the P.D.E.-J.B. inversion. As is to be expected by the smaller residuals calculated by the plane wave method, contrasts in the plane wave inversion are smaller, about 2.5 percent or 0.15 km/sec. The mantle layers show a velocity structure that decreases in the northeastern direction. This structure is rather different from the crustal layer, although the high velocity regions in the northwest quadrants of the crust and upper mantle seem to be part of the same structural unit. A northwesterly trending low velocity zone appears in both inversions and in all three mantle layers. This structure is not vertical, but rather dips to the northeast at about seventy degrees. Since the inversion is subject to some vertical smoothing, the actual vertical extent of this structure is probably less than observed, or about 80 Km. The fourth layer of the inversion, although still showing the same general trends of the upper two mantle

layers, shows more small scale inhomogeneties. These are taken to be noise.

By constructing a three dimensional laterally varying velocity structure for the Tarbela area, 55 percent of the observed data variance (the summed squares of the travel time residuals) can be accounted for. This reduces the residuals to approximately the 0.1 second resolution limit caused by limited accuracy in reading the original seismograms.

Implications of this velocity structure to geologic structure in the Tarbela area, and to Himalayan tectonics will be discussed below.

Table One

The Initial Model Used in the Tarbela Inversion

<u>Layer #</u>	<u>Velocity (km/sec)</u>	<u>Thickness (km)</u>	<u>Depth of Center (km)</u>
1	6.1	33	15
2	7.8	40	45
3	7.8	40	85
4	7.8	40	125

Table Two

The Results of the Inversions

<u>Method</u>	<u># of events</u>	<u># of obser- vations</u>	<u>data variance (sec²)</u>	<u>residual variance</u>	<u>% improve- ment</u>	<u># of blocks observed</u>
PDE - JB	122	991	0.043	0.0192	55.	229
plane wave	122	991	0.021	0.0096	55	226

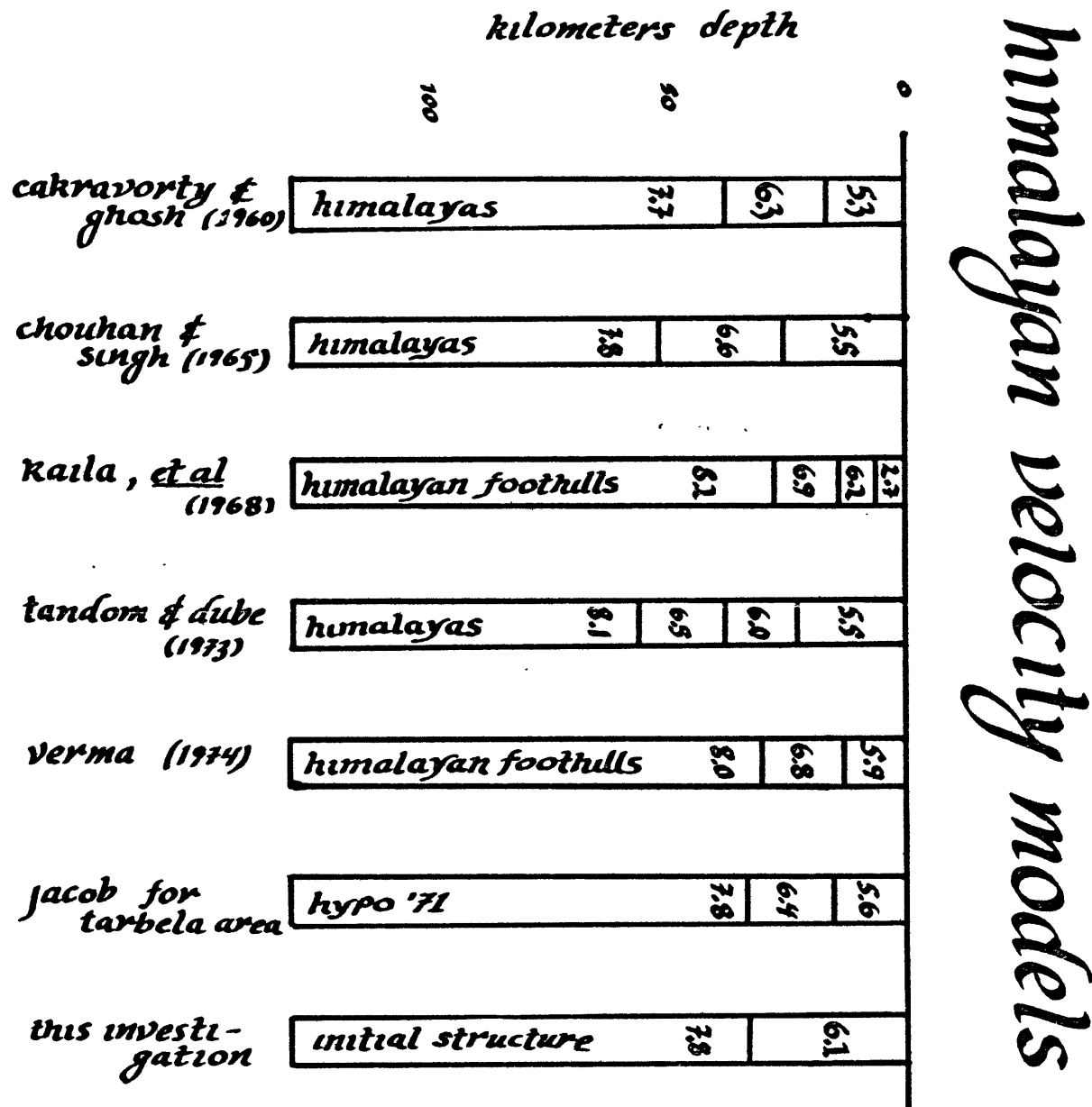
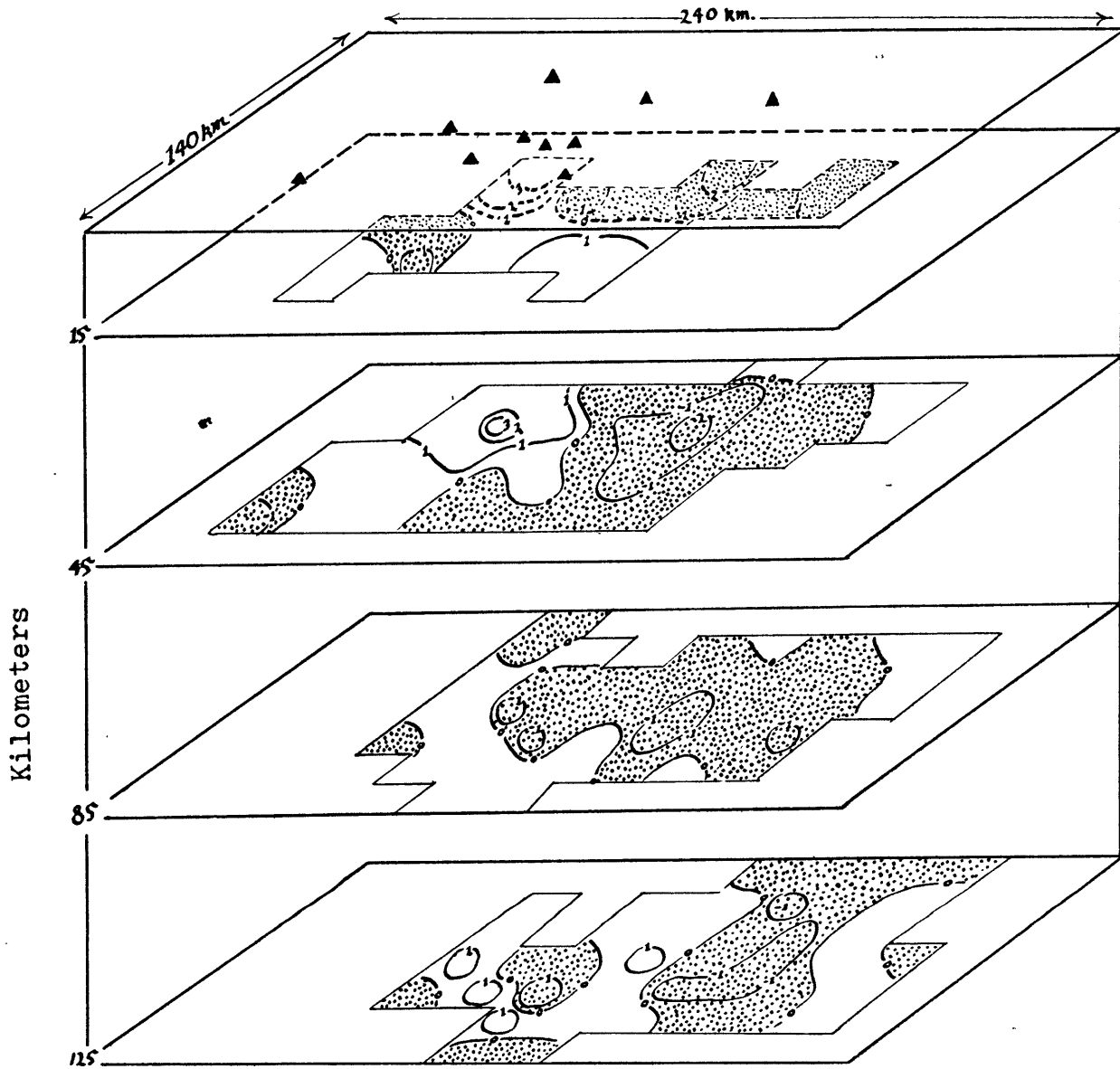


Figure 8 : A comparison between some recent plane layered Himalayan velocity models and the initial model used in the inversion. Note the similarity between the Himalayan Foothill and Tarbela area models. The initial model used in the inversion is a simplified Tarbela area model.

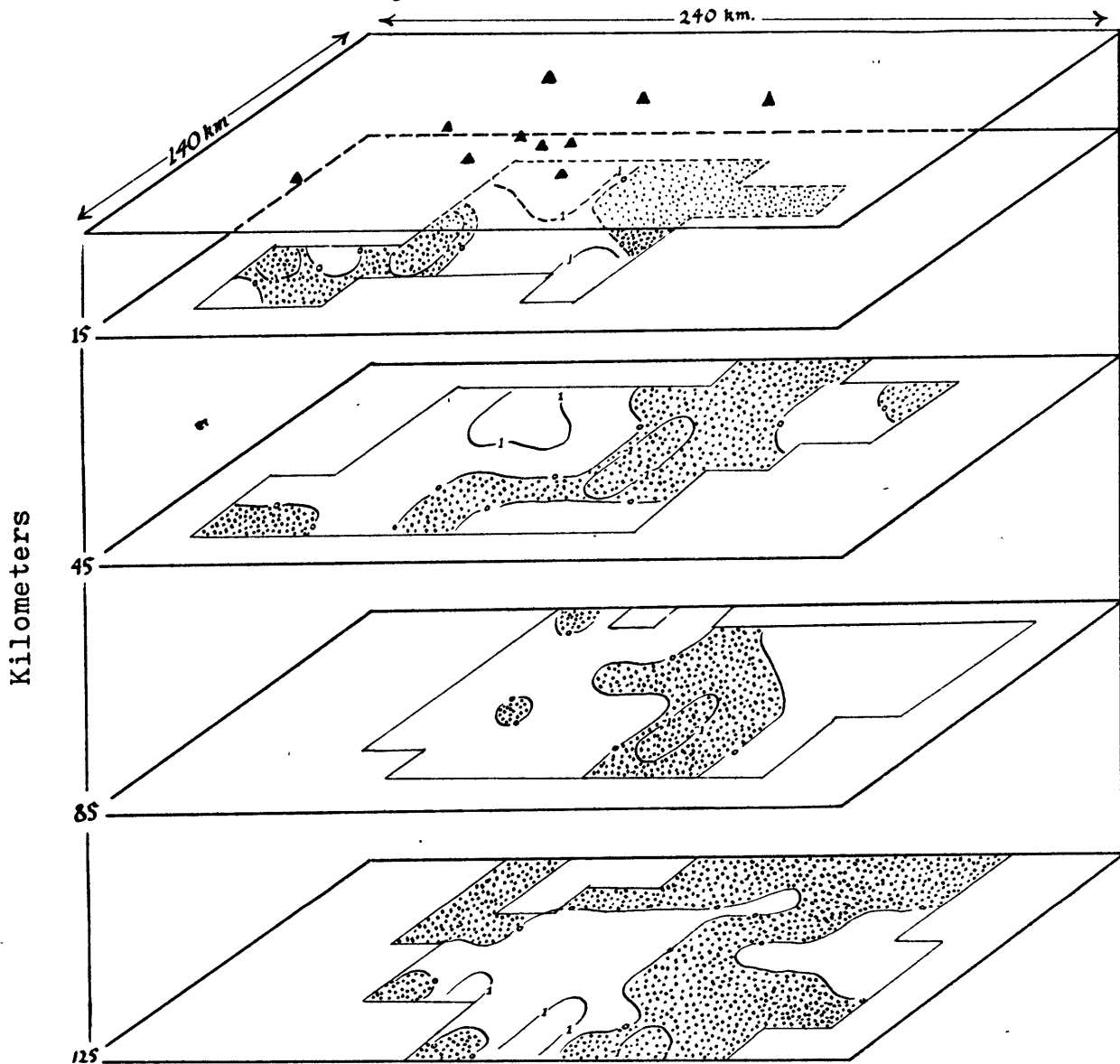
Tarbela array P-velocity structure p.d.e.-j.b. method



vertical exaggeration 2:1 contoured in percent of average layer velocity

Figure 9 : Final inversions of the P.D.E.-J.B. (this page) and the plane wave (next page) relative travel time residual data. Triangles on the top of the inversion are the stations used in the inversion. All contours are in percent above and below the average layer velocity (see table one). Velocity anomaly magnitudes for each layer are determined only up to a constant.

Tarbela array P-velocity structure plane wave method



vertical exaggeration 2:1 contoured in percent of average layer velocity

Figure 9 (con't).

Figure 10 (next 10 pages)

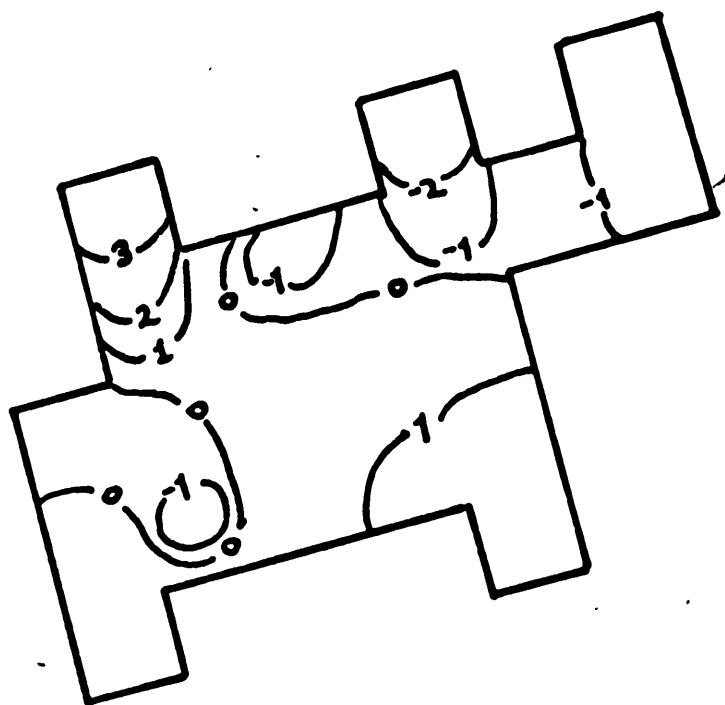
Final inversion of the Tarbela data contoured in percent above and below the average layer velocity. The four layers of the P.D.E.-J.B. inversion are labeled with the letters PDE followed by the layer number. In a similar manner the layers of the plane wave inversion are labeled with PW. These contour maps can be overlaid on the geologic or seismicity maps.

Geology within the blocked in area of the map is taken from a detailed map prepared by Calkins, et al (1972). Formations outside the blocked region have been sketched off a much less accurate map of Himalayan geology prepared by the United Nations (1971).

Triangles on the seismicity map show the locations of the stations of the Tarbela array. Small circles are recent seismic events. The loop in the thrust fault is the Hazara Syntaxis. Note the correspondence of the trend of the velocity anomalies in the inversions and the trend of the zone of intense seismicity in the top center of the map. These features are nearly parallel.

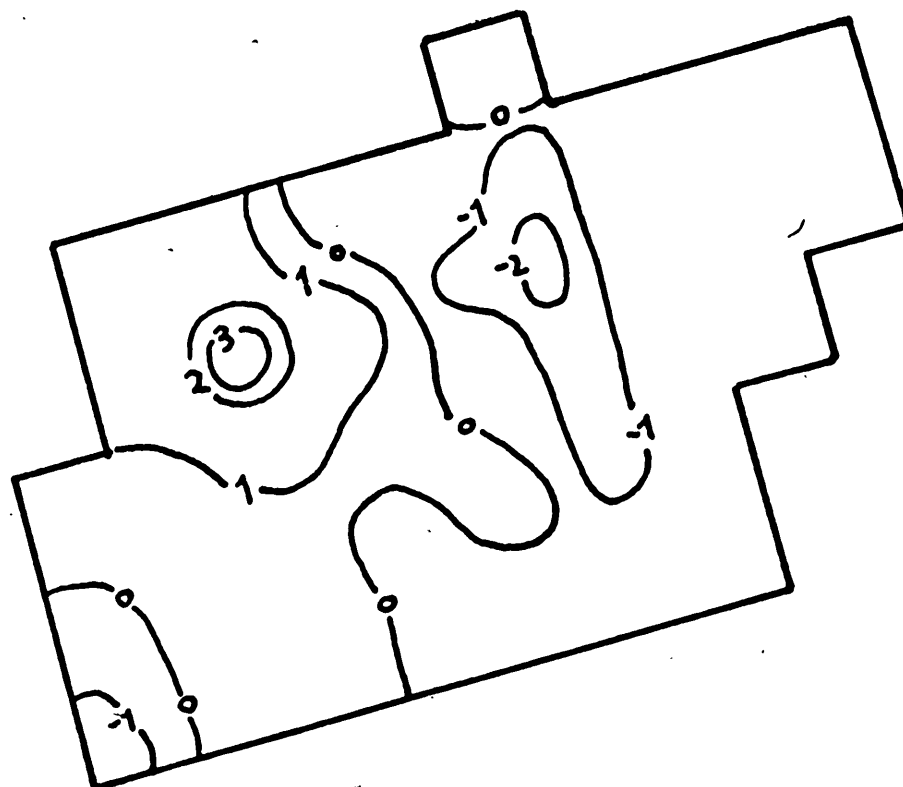
Depth = 15 km

pde 1



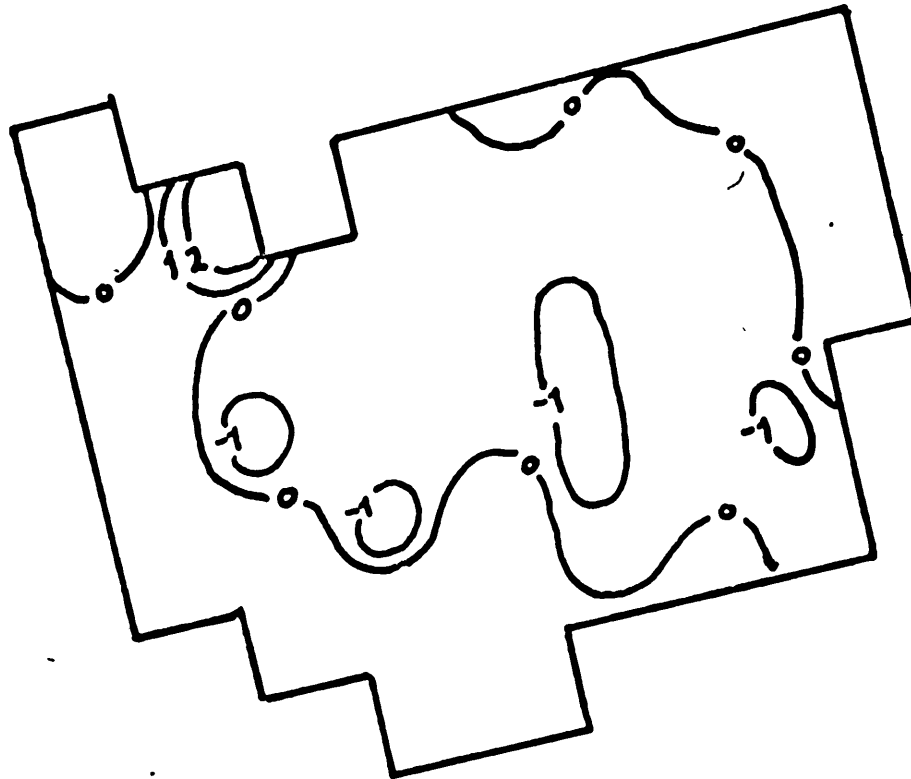
Depth = 45 km

pde 2



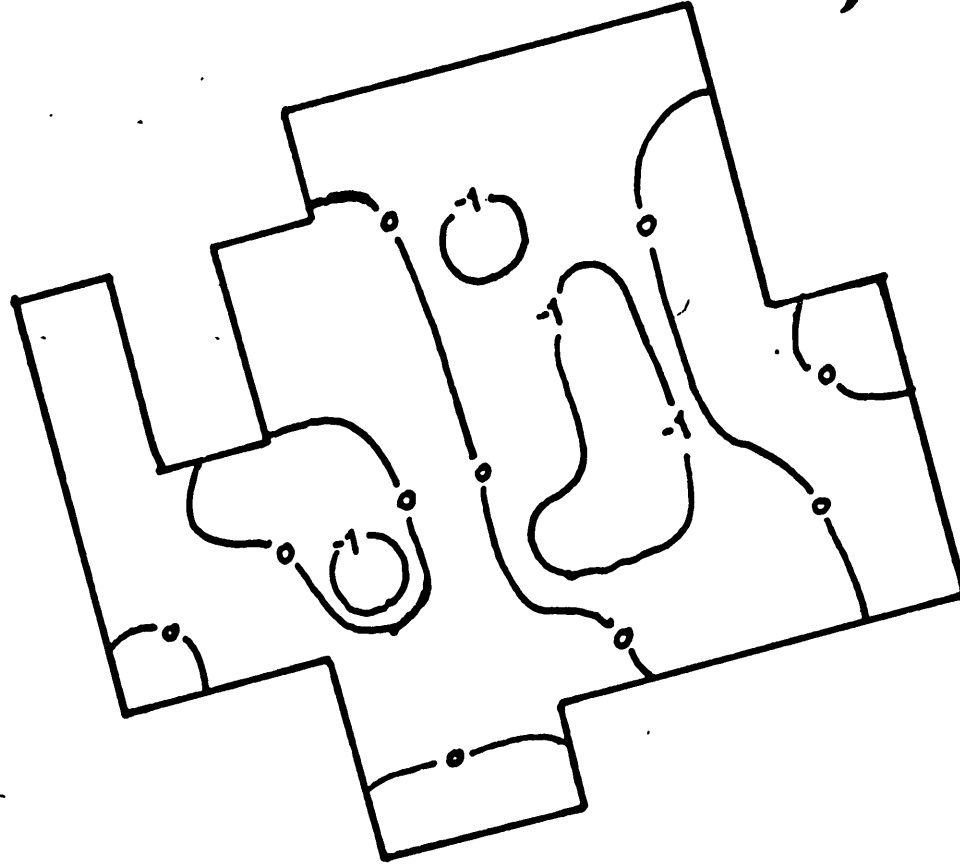
depth = 85 km

pdf 3



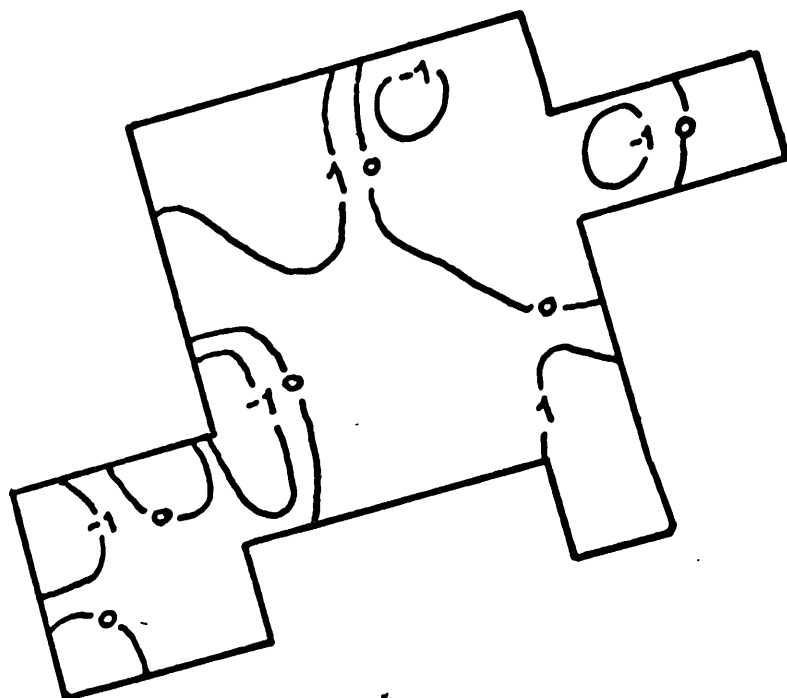
Depth = 125 km

pde 4



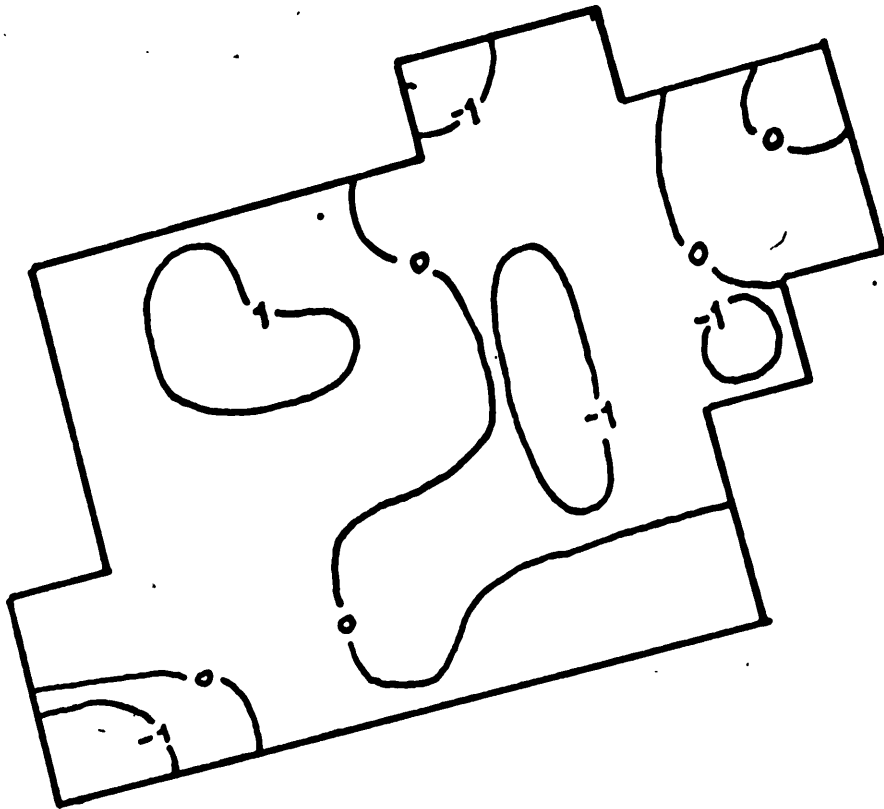
Depth = 15 km

pw 1



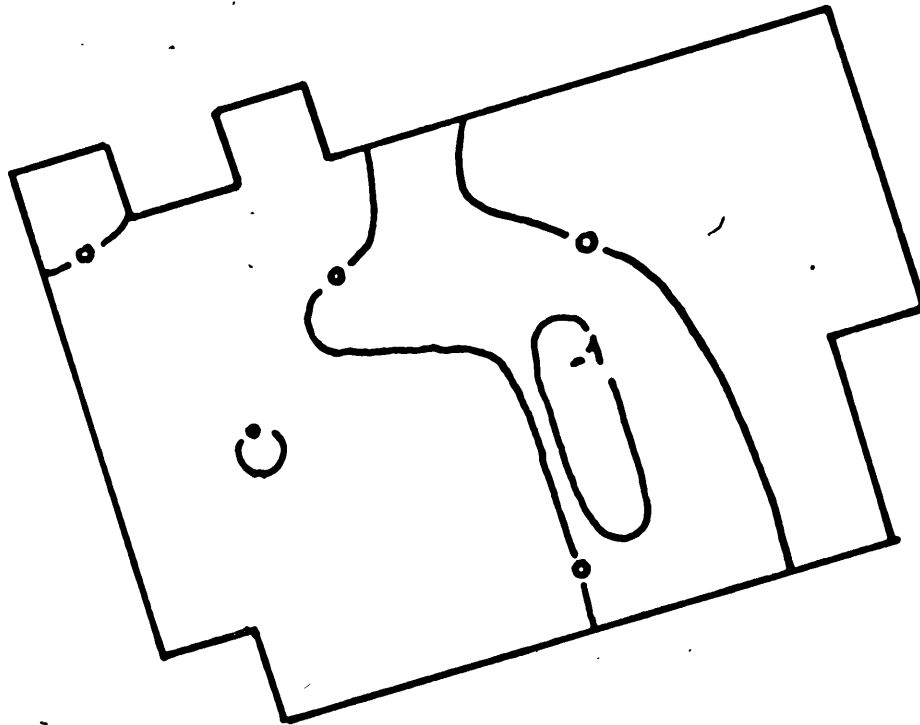
Depth = 45 km

pw 2



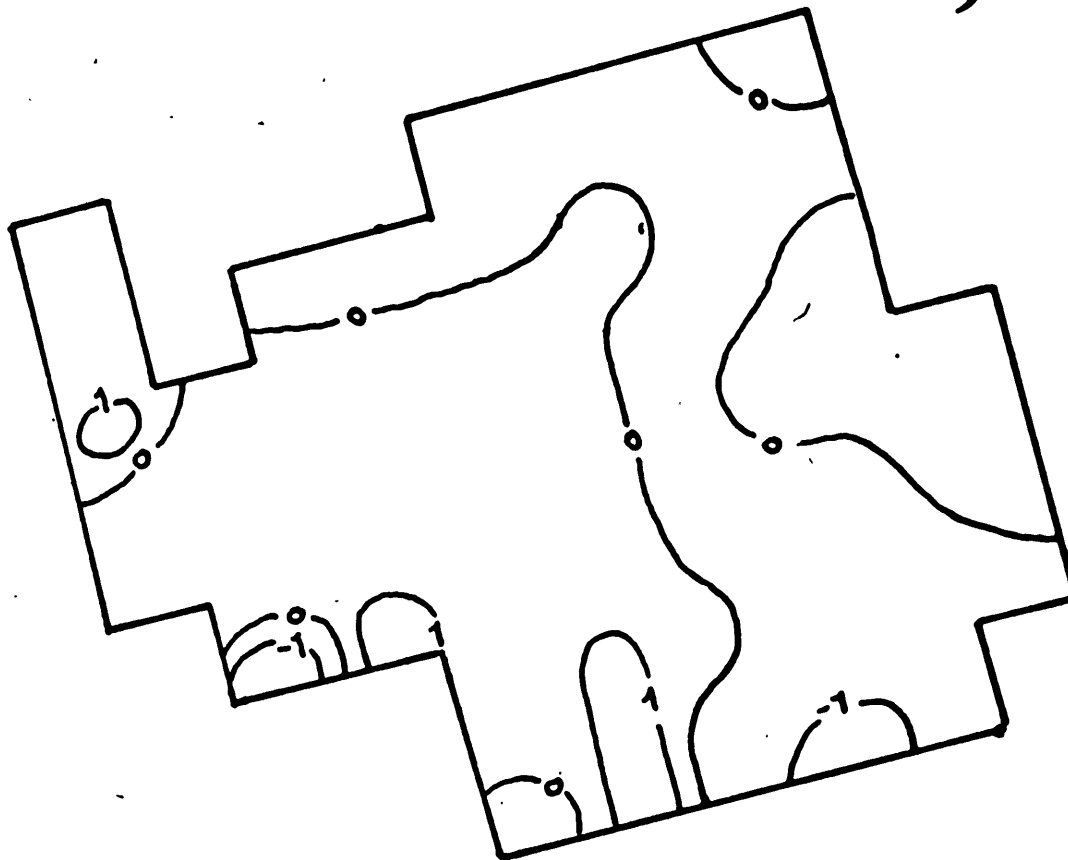
• Depth = 85 km.

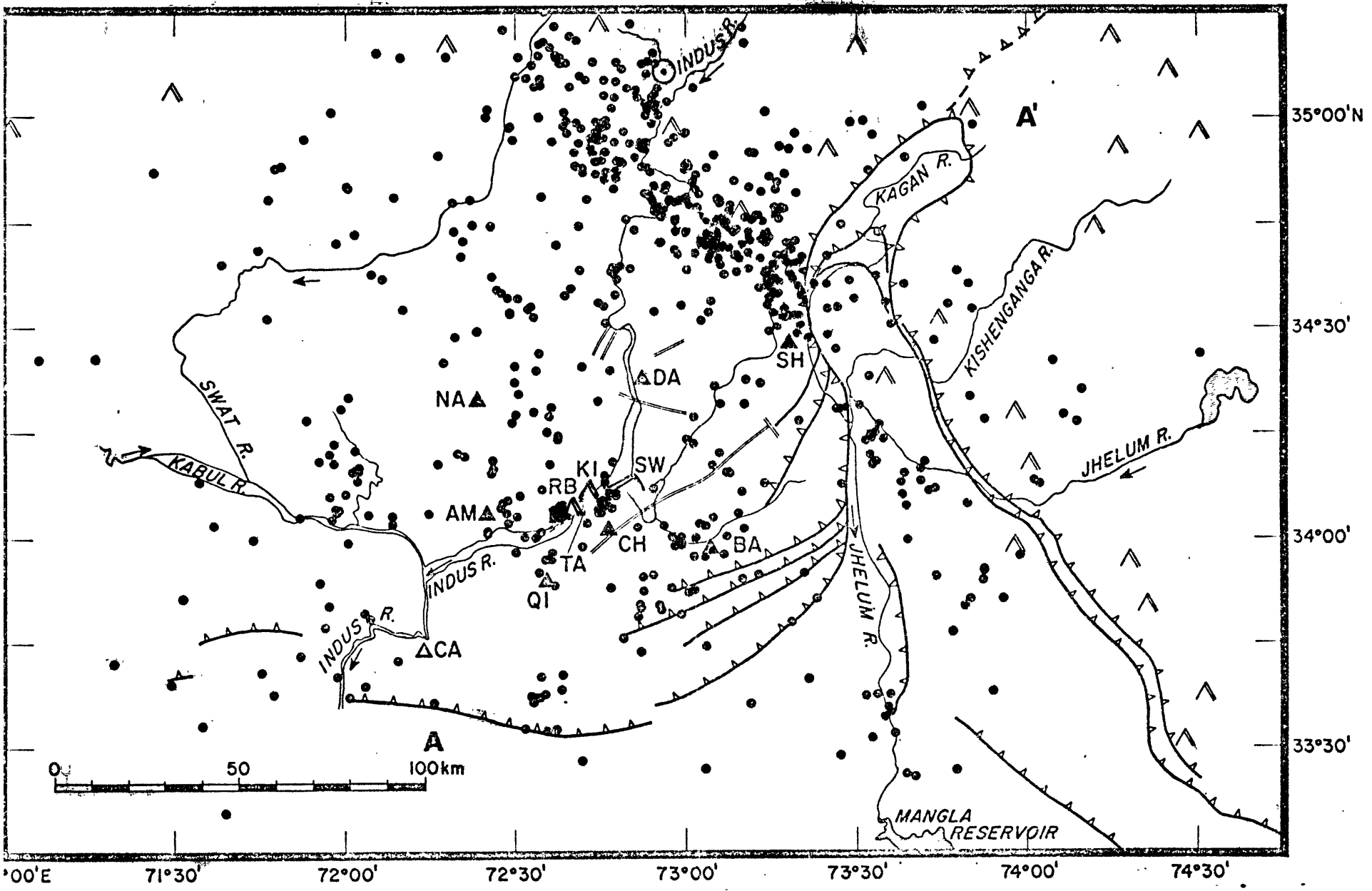
pw 3

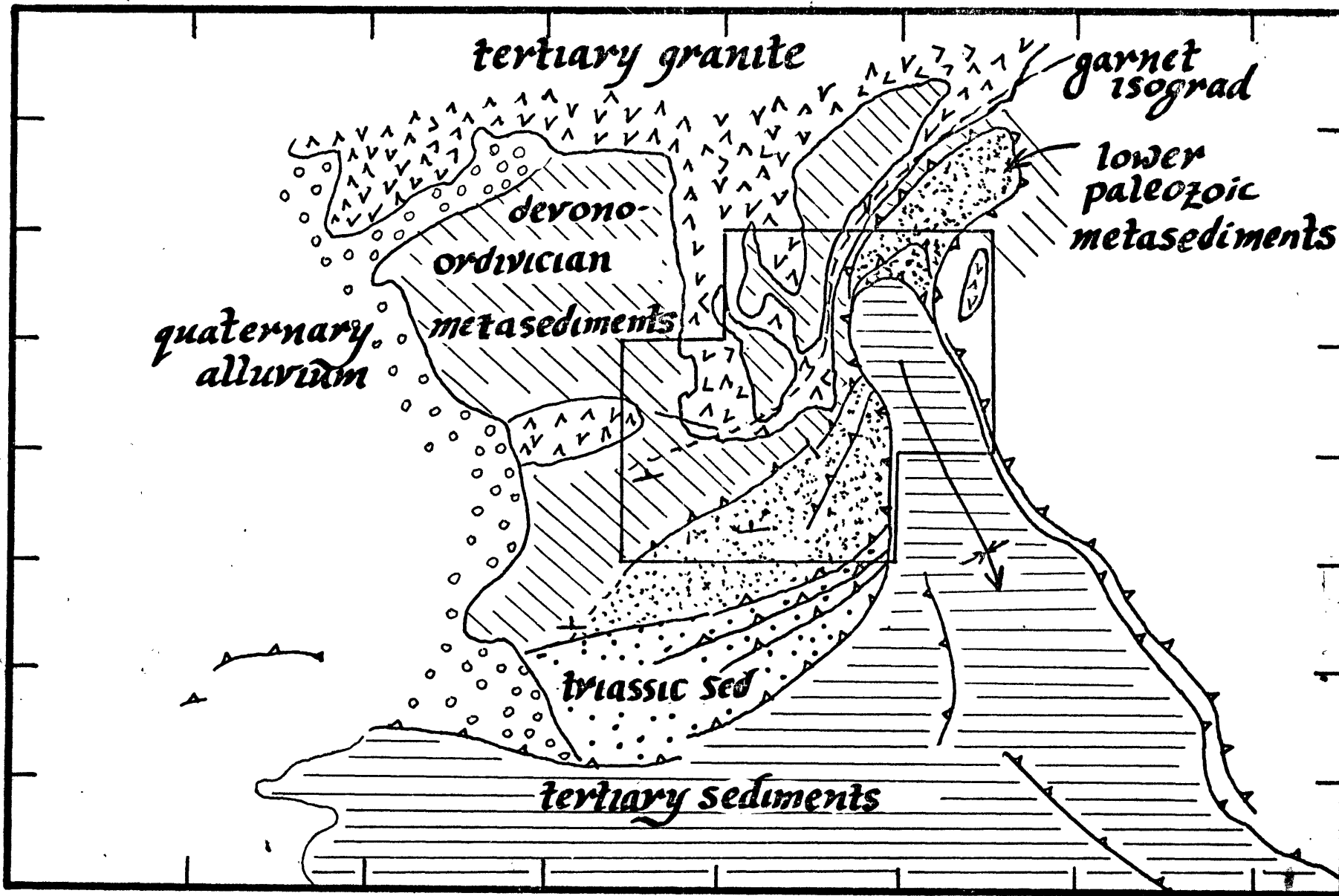


Depth = 125 km


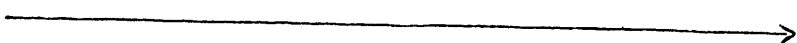
pw 4







Implication to Geologic Structure

In discussing the implication of the Tarbela inversion to geologic structure in that area it is first necessary to consider evidence that such an inversion actually closely approximates the  existing structure. While this is the original intent of the inversion, the question is by no means unimportant or trivially answered. A variety of factors, including assumptions regarding the applicability of ray theory, the station configuration, and the data quality are involved in providing a satisfying answer. To examine the reliability of the inversion method a series of experiments were performed wherein data corresponding to a known structure were inverted. . Such an inversion was performed using a block configuration similar to that used in the Tarbela inversion, using synthetic data created for a Tarbela-like array. The method of creating these data is given in Appendix One and the inversion of it in Appendix Two. Satisfactory results were obtained although some vertical smoothing of structures occurred.

Granting that the velocity structure observed by the Tarbela inversion closely resembles the actual Tarbela structure, it is necessary to consider the causes of observed inhomogeneties. Four factors predominate in controlling the P wave velocity. These are the composition of the rocks,

the number of cracks per unit volume, the temperature of the rocks, and their degree of weathering. Relatively unconsolidated, cracked, hot, or weathered rocks have the lower velocities. Of these four factors any one can have a roll in determining or modifying the velocity of the crust. The isolation of the mantle from the weathering processes of the surface and the pressure at that depth suggest that weathering and cracks are of secondary importance there.

The Crust

In examining Figure 10, by overlaying layer 1 of the P.D.E.-J.B. inversion on the geologic map, little correspondence can be found between the boundaries of geological formations and the contours of the crustal inversion. Nor is any single formation consistently high or low, with the exception of the Tertiary granite which lies completely in the northeastern, low velocity quadrant of the overall saddle shaped crustal velocity structure. Although the age of this granite suggests that it is cool, the consistent decrease in velocity toward the central portions of the granite body could reflect residual heat in those portions. More probable, as was suggested by Calkins, et al (1972) this granite is associated with partial melting above the thrust zone. It therefore ranges from zero thickness at the fault trace to several kilometers thick at the

array edge. In this case the granite, as well as other portions of the upper thrust sheet, contribute only slightly to perturbations found in the crust. The inversion is actually yielding information about the lower thrust plate. The northwestern trend of the ridge of the saddle is approximately parallel with the trend of the Main Boundary Thrust southeast of the Hazara Syntaxis, and with the zone of intense seismicity northeast of the Syntaxis. This trend, and its counterpart in the mantle (which will be discussed below) suggest that the overall tectonic picture of the crust in the Tarbela area is much the same as for regions to Tarbela's southwest. These features maintain a northwest strike, unlike the surface features observed in the vicinity of the syntaxis.

The Mantle

The inversion of the P.D.E.-J.B. data (which contains the most information of the two data reduction schemes used) shows a general decrease in velocity across the array area to the northeast. This trend is evident in all three layers of the mantle inversion, although most prominent in the upper two. The observed gradient is the manifestation in the inversion of the regular shift in the ray parameter vector, which has previously been interpreted as a northeasterly dipping Moho having northwest strike. Since the lower thrust plate causes a thickening of the crust towards the northeast, and a depressing of

velocity contours in that direction, each layer in the inversion shows this decrease, although it is most prominent in the uppermost layer. The elongated low velocity anomaly that is clearly present in all three mantle layers is a feature which also strikes in the northwest direction. Its relatively small horizontal width and considerable vertical extent (at least 80 kilometers) raise difficult questions as to its interpretation. One explanation is to postulate a zone of normal faulting associated with the downward flexing of the lithosphere in the area. The lack of any seismic activity correlatable with this feature provides no supporting evidence for such a conjecture. More likely is the possibility that this feature is due to a high temperature zone associated with magmatic intrusion in this confined area. The seventy degree dip of the anomaly implies either emplacement at that angle or deformation of the lithosphere to produce such a dip from an originally vertical one. Such deformation is to be expected in a down-thrusting lithosphere, since the top surface, in experiencing drag from the upper plate, is slowed down relative to the bottom of the lithosphere, which is presumably closer to the driving mechanism of the plate. Shear deformation of the lithosphere takes place. In either case the suggestion of magmatic intrusion at this depth is a surprising one since a source of heat and magma must be postulated below the thrust zone of the Main Boundary Fault. One plausible

source of such heat and magma is from motion (aseismic motion in this region because of the constraints of local seismicity) along a deeper thrust zone. Such a zone would constitute the youngest of a series of three imbricated thrusts, the other two of which outcrop to the north : the Main Boundary and Main Central Thrusts. The new thrust zone would presumably outcrop to the south of Tarbela. No such outcrop is observed, but recent tectonic models of the Himalayas (see for instance LeFort (1975)) as well as weak seismic evidence (see for instance Menke and Jacob (1976)) suggest that the idea is viable. The author does not intend to assert that the observed velocity anomaly is sufficient evidence to conclude such thrusting and frictional melting is taking place. Yet it is plausible that such melting would tend to occur at a specific depth along the strike of the thrust, leading to a velocity anomaly of shape similar to the observed anomaly.

Conclusions

Although surface geology suggests that the Main Boundary Fault bends southward to join the strike-slip faults of the Baluchistan Arc, the deep structure, as learned through the Tarbela inversion, indicates that the bulk of the lithosphere maintains the general northwest strike found in more central parts of the Himalayas. Since the Main Boundary Thrust is expected to eventually join some northerly trending strike slip fault, we are led to conclude that it must join such a fault ^{located} considerably to the northwest of Tarbela. A likely candidate is the Quetta Chaman Fault, which is located several hundred kilometers west of the Baluchistan Arc. Tectonic evidence, and to a lesser extent seismic evidence (see for instance, Molnar and Tapponnier (1975)) suggest that considerable motion takes place on this fault. The surface structures found around the Tarbela area, and perhaps some of the northern Baluchistan Arc as well, are to be understood as shallow features not governed by the overall tectonics of the region. They were formed by secondary processes perhaps including gravity slumping from higher elevations to the northwest.

Appendix One

Semi-Analytic Travel Time Residual Calculation for Simple But Non-Trivial Geometry

An algorithm for calculating travel time residuals for a plane wave impinging upon a sphere of radially symmetric velocity distribution imbedded in a homogeneous half space is presented below. Such an algorithm, though it can be thought of as modelling geologic structures such as batholiths, is useful mainly in that semi-analytic solutions to the ray path equations can be found, atleast for specific (but non-trivial) velocity distributions. The high accuracy and low cost of such a method make it useful in providing synthetic data corresponding to a known structure, by way of which inversion procedures can be tested. A test of the inversion method used in the Tarbela study will be made below.

The chief virtue of choosing a spherically symmetric velocity anomaly is that raypaths from a plane wave to points (ie. geophones) above the sphere are cylindrically symmetric about an axis which passes through the sphere's center and which is also normal to the plane wave. Choosing to work in this cylindrical coordinate system, whose orientation is determined by the azimuth and ray parameter of the plane wave, reduces the problem to one independent of polar angle, and thus to a two dimensional problem.

After choosing the velocity to be continuous across the sphere's surface (which can always be done since a small shell of the half space can be included as part of the velocity anomaly), the condition that a ray start normal to the plane wave and pass through the point at which the geophone is located is given by (see Figure 1) :

$$f(\alpha) = \alpha + i(\alpha) + \Delta(\alpha) - \pi = 0$$

where : α : angle between the z axis and the exit point of the ray from the sphere

$i(\alpha)$: angle of incidence of the ray with respect to the sphere's normal

$\Delta(\alpha)$: angle between the entry and exit points of the ray and the sphere's center.

These functions are, by simple geometry and spherical ray theory :

$$i(\alpha) = \alpha - \tan^{-1} \left(\frac{r_g - R_s \sin \alpha}{z_g - R_s \cos \alpha} \right)$$

where : R_s : radius of the spherical velocity anomaly

r_g, z_g : cylindrical coordinates of the geophone,

$$\Delta(\alpha) = 2p \int_{R_b}^{R_s} (\eta^2 - p^2)^{1/2} dR$$

where : p : ray parameter relative to the sphere

η : slowness

c : velocity

R : radial distance to sphere's center

R_b : bottoming radius of ray in sphere

and :

$$p = \eta(R_s) \sin i(\alpha)$$

$$\eta = R/C(R)$$

$$R_b = p C(R_b)$$

In the case of a monotonically increasing velocity distribution within the sphere, limits can be placed on the parameter alpha. The minimum alpha is associated with a line that is normal to the sphere and which passes through the geophone. If the geophone is not geometrically shadowed by the sphere (ie. r_g greater than R_s) the maximum alpha is associated with a line that is tangent to the sphere and which passes through the geophone. In the case where the geophone is shadowed the maximum alpha is associated with a line that is parallel to the z axis and which passes through the geophone (see Figure 2) . Then :

$$\alpha_{min} = \tan^{-1}(r_g/z_g)$$

$$\alpha_{max} = \begin{cases} \sin^{-1}(r_g/R_s) & r_g < R_s \\ \alpha_{min} + \cos^{-1}\left(\frac{R_s}{(r_g^2+z_g^2)^{1/2}}\right) & r_g \geq R_s \end{cases}$$

If no zero to the function f can be found within the above limits, then no ray passes through the sphere and connects the geophone to the plane wave.

Once the correct alpha has been found the travel time through the sphere is given by :

$$t_{sph} = 2 \int_{R_b}^{R_s} \frac{n^2 dR}{R (\eta^2 - p^2)^{1/2}}$$

The travel time for the entire 'refracted' ray is given by adding the contribution of the top and bottom straight portions of the ray path to t_{sph} . The starting time is arbitrarily taken to be the time when the plane wave reaches the bottom of the sphere. Then:

$$t_{bot} = R_s (1 - \cos(\pi - \alpha - \Delta)) / C(R_s)$$

$$t_{top} = \left[(z_g - R_s \cos \alpha)^2 + (r_g - R_s \sin \alpha)^2 \right] / C(R_s)$$

$$t_{ref} = t_{bot} + t_{sph} + t_{top}$$

In the case when r_g is greater than the radius of the sphere, no shadowing of the geophone from a direct ray takes place. The travel time of the direct ray is given by :

$$t_{dir} = \frac{R_s + z_g}{C(R_s)}$$

The travel time for the first motion is given by the smaller of the direct and refracted ray travel times.

Travel time residuals can then be calculated by a method analagous to the P.D.E.-J.B. method used in the Tarbela study. The travel time for the direct ray is calculated from the expression given above whether or not it actually exists, and its time subtracted from the actual travel time. Relative residuals are then constructed by

removing the mean residual. Plane wave residuals can also be calculated by fitting a plane wave to the arrival time data.

If the velocity in the sphere is chosen to be

$$C(R) = a - bR^2$$

where a, b are real positive constants, then rays passing through the sphere have a constant radius of curvature

given by :

$$\rho = (2b\rho)^{-1}$$

Since at the exit point _A^P of the ray from the sphere (see Figure 3) the slope of the ray (in the cylindrical coordinate system) is known (it is the same as the slope of the straight ray in the upper portion of the half space), the coordinates of the circle's center can be calculated as a function of alpha. The equation of the raypath through the sphere is :

$$r_p = w - (\rho^2 - (z_p - u)^2)^{1/2}$$

The ray's center of curvature is at (u, w). The ray's slope is:

$$r'_p = \frac{dr}{dz} \Big|_{z_p} = (z_p - u) (\rho^2 - (z - u)^2)^{-1/2}$$

Since the slope at point P is known to be :

$$r'_p = (r_g - R_s \sin \alpha) / (z_g - R_s \cos \alpha)$$

the above equations can be solved to yield :

$$u = R_s \cos \alpha - r'_p \rho (1 + r'^2)^{1/2}$$

$$w = R_s \sin \alpha + [\rho^2 - (R_s \cos \alpha - u)^2]^{1/2}$$

Then :

$$\frac{\Delta}{2} = \tan^{-1} \left(\frac{w}{u} \right) - \alpha$$

$$R_b = (w^2 + u^2)^{1/2} - \rho$$

Since the function f now contains only elementary functions of the parameter α , its zero can be calculated by simple numerical methods.

Once the appropriate α has been determined, travel time through the sphere can be numerically determined by integrating the travel time $ds/C(r)$, where ds is the arc length, over small segments of the now known ray path. In practice the raypath can be divided into many small arcs, and the velocity over any arc taken to be the velocity at the arc's midpoint.

Synthetic travel time residuals were calculated for the stations of the Tarbela array by the method described above. The half space was assigned a velocity of 6.0 km/sec which increases quadratically to 6.6 km/sec at the center of the anomalous sphere. This sphere was located at a depth of 30 kilometers beneath the array's center and had a radius of 25 kilometers. Graphs of residuals vs. azimuth are shown in Figure 4 for several choices of ray parameter. The inversion of this synthetic data is discussed in Appendix Two.

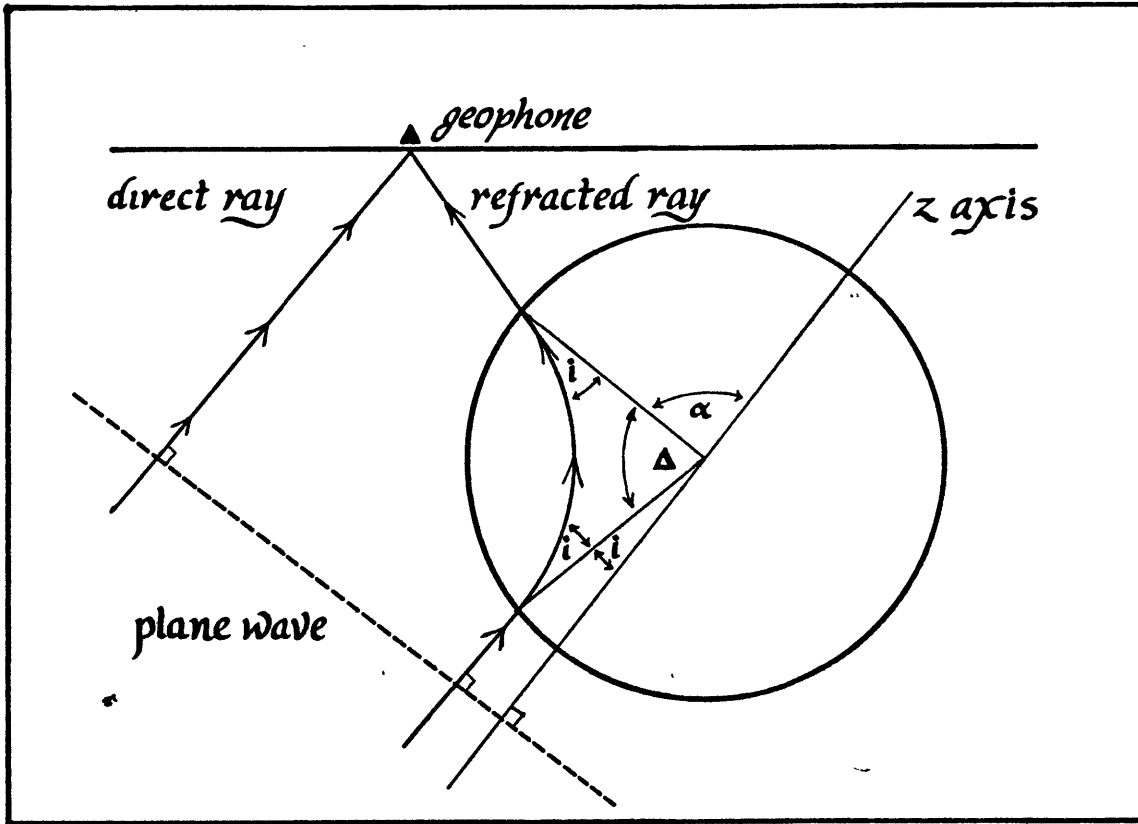


Figure 1 : Refracted ray reaching geophone after passing through the spherical velocity anomaly.

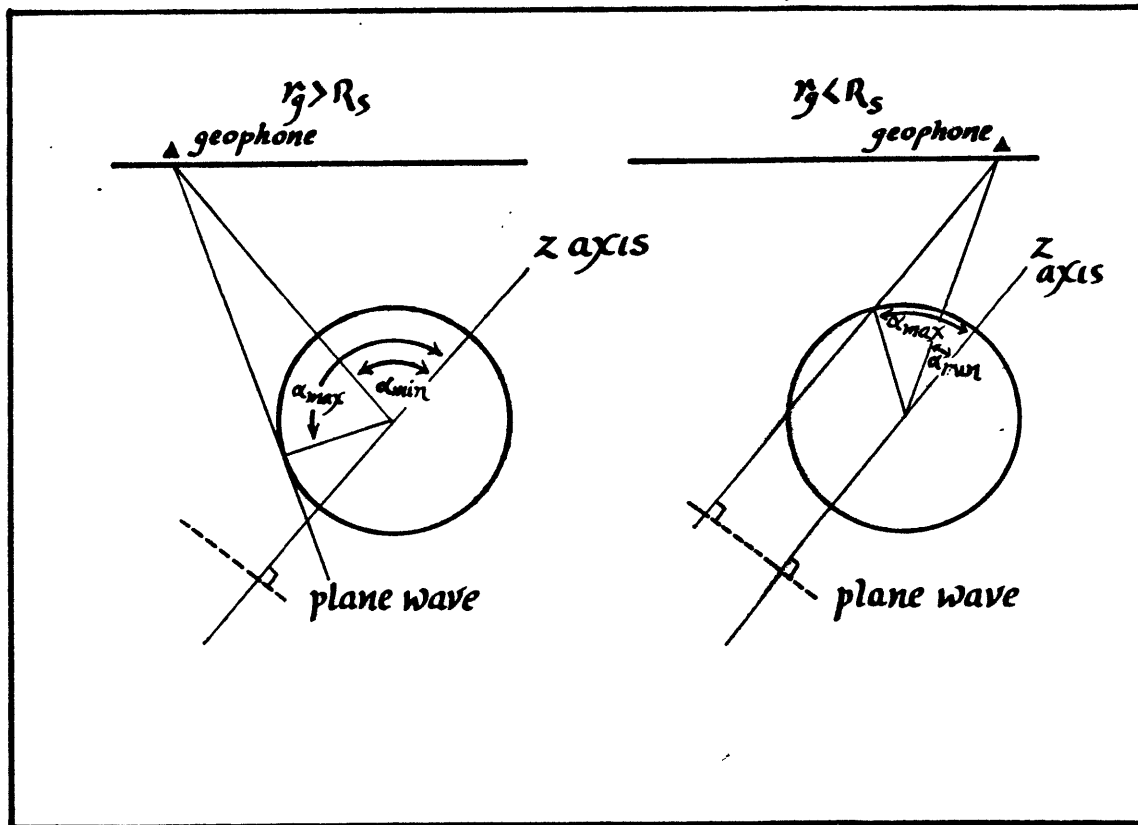


Figure 2 : Limits of the parameter alpha.

57

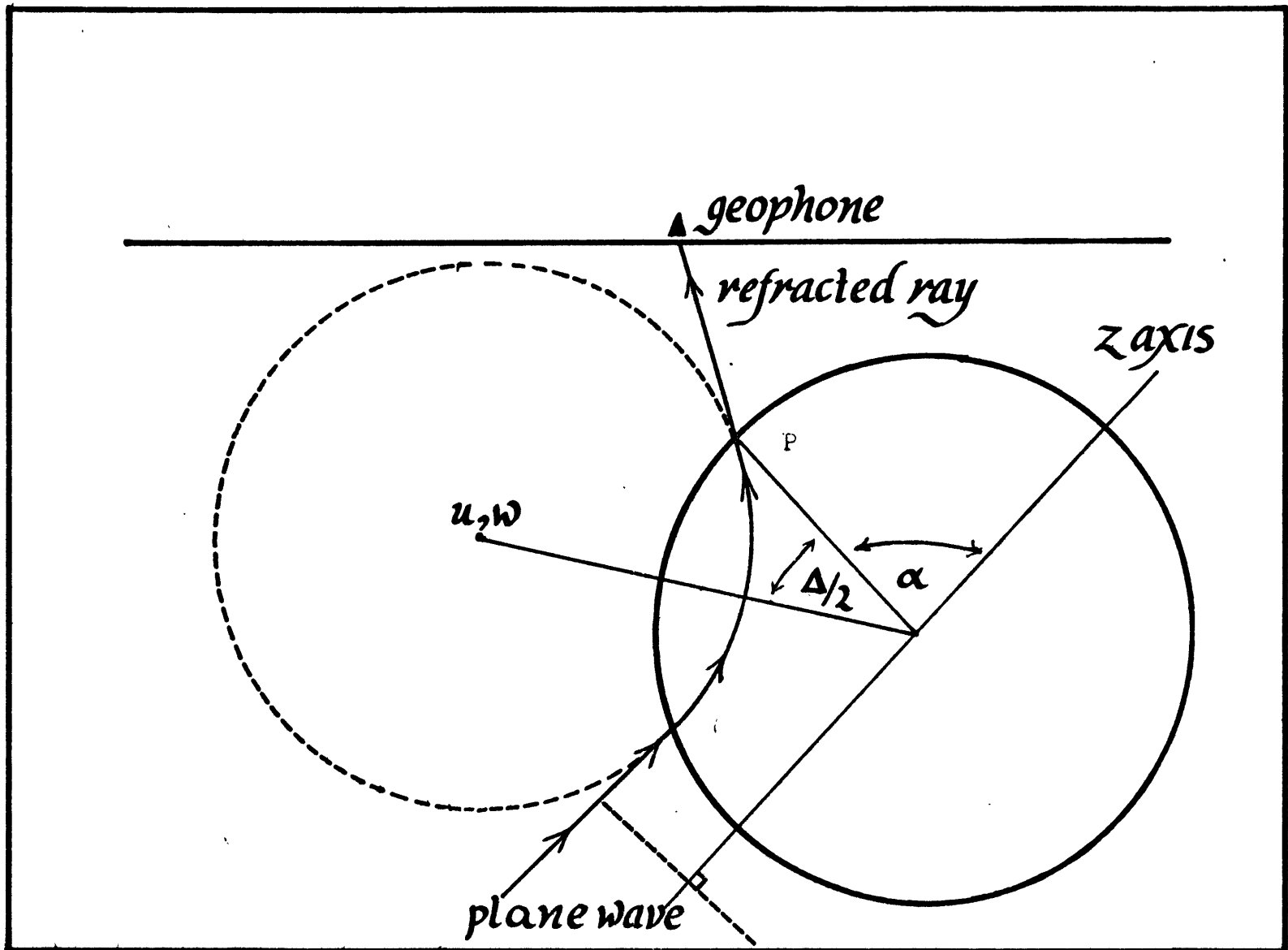


Figure 3 : When the velocity anomaly is spherically symmetric and has a velocity distribution that quadratically increases toward the sphere's center, the ray path is a circular arc whose center, at (u, w) can be easily determined, as a function of the parameter α .

Synthetic Travel Time Residuals

"p.d.e. - j.b." plane wave

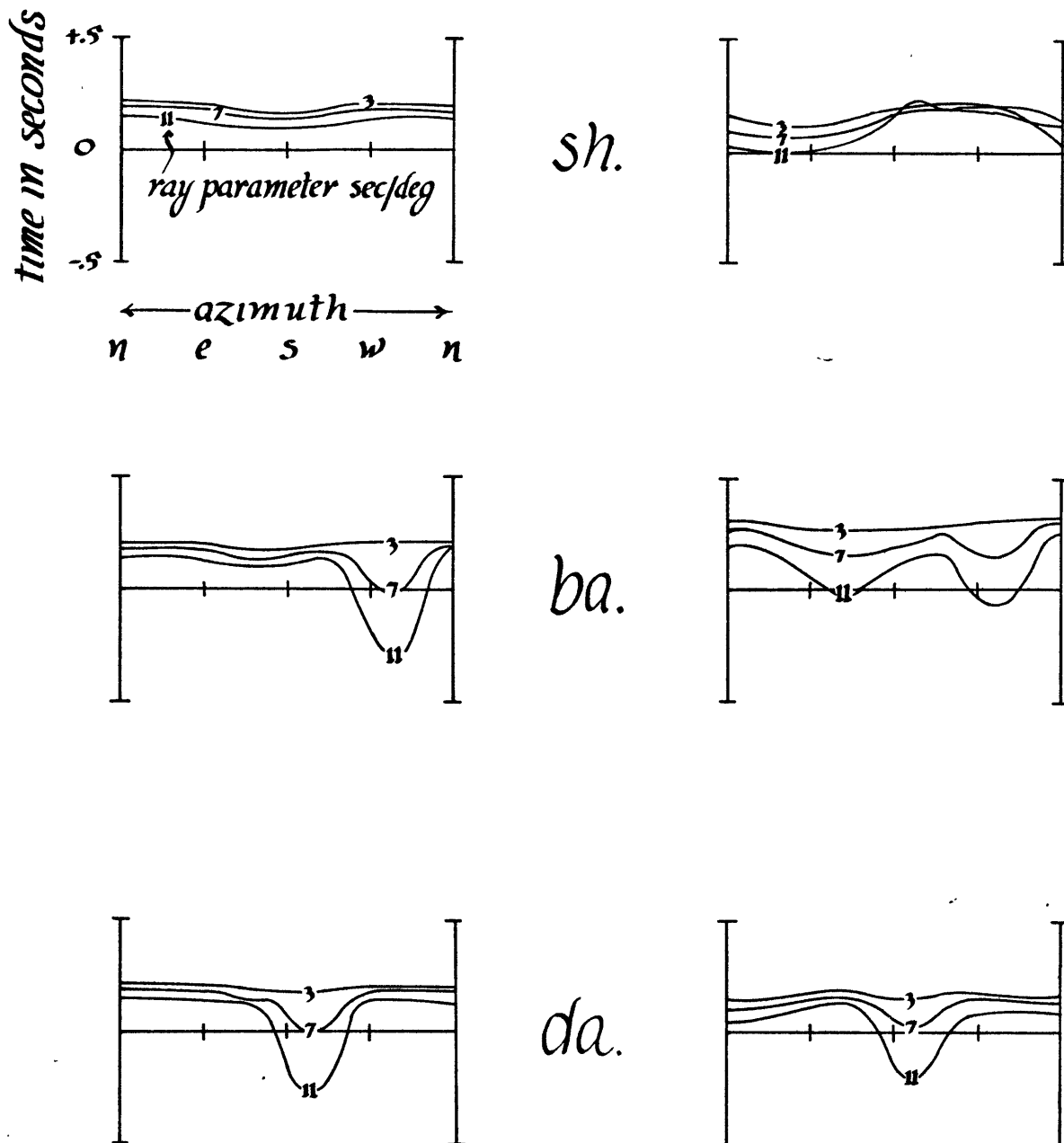


Figure 4 : Relative travel time residuals plotted against azimuth for an artificial situation where the stations of the Tarbela array are located above a single spherical velocity anomaly located within an otherwise homogeneous half space. To the left of each station mnemonic (sh,ba,qi, etc.) (continued on next page)

Synthetic Travel Time Residuals cont'd

"p.d.e.-j.b." plane wave

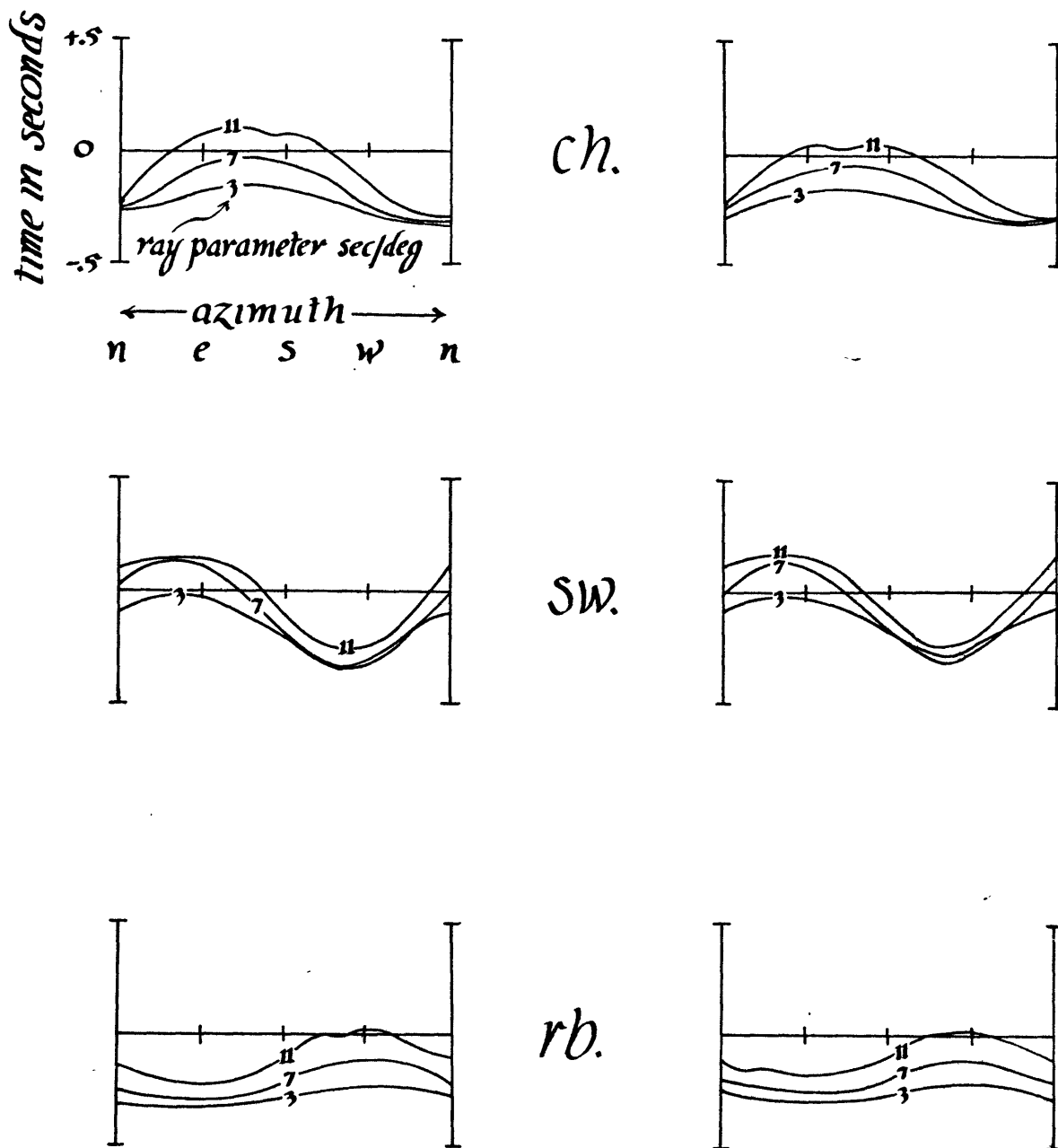


Figure 4 (con't) : synthetic arrival time data is processed by the 'P.D.E.-J.B.' method. To the right data is processed by the plane wave method. Curves for three choices of ray parameter are given. Notice that the larger ray parameters (and shallower angles of incidence) are associated with the larger residuals. Shallower rays encounter the more widely different areas of the velocity distribution beneath the array.

Synthetic Travel Time Residuals cont'd

"p.d.e. - j.b." plane wave

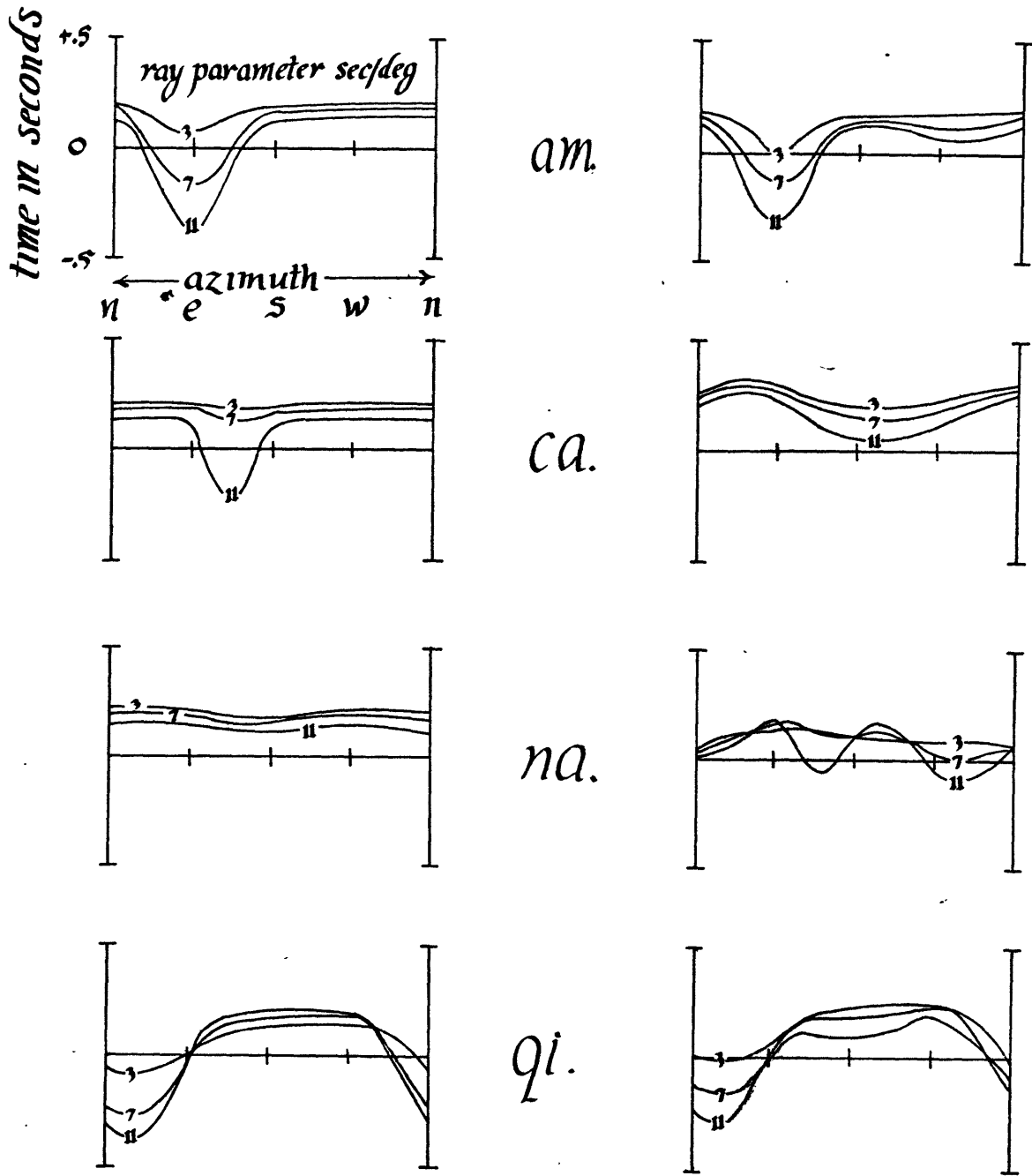


Figure 4 (con't),

Appendix Two

Inversion of Synthetic Travel Time Residual Data

In order to examine the reliability of the inversion method used in the Tarbela study, synthetic data corresponding to a sphere imbedded in a homogeneous half space was inverted for the station and block configuration of the Tarbela network. Four tests of the inversion were run, corresponding to processing the data by the "P.D.E.-J.B." and plane wave methods for two choices of data coverage. More information about this data is given in Table 1 and in Appendix One. All data had one of three ray parameters, corresponding to near, intermediate and very distant (PKP) events.

The most accurate inversion was obtained in Case A (see Figure 1A and Table 2), where all synthetic data for the "P.D.E.-J.B." case was used. Examination of Figure 1A shows that the spherical velocity anomaly, 25 kilometers in radius and centered at a depth of 30 kilometers, has been successfully located on the first three layers of the model. The maximum contrast is about 8 percent, somewhat lower than the actual contrast of 9 percent, but reasonable since that contrast is found at only a small volume at the sphere's center. Layer four, which should be free of velocity contrasts since it is below the level of the sphere, shows a pattern of residuals remanescant of the sphere. Structure has been projected downward to this level. However con-

trasts on this layer are smaller than on the upper three layers, a maximum of about two percent. Layer five shows no obvious structure and has very low contrast. The maximum contrast on layer five is about one percent, but the average is much closer to 0.5 percent. Layer five contrasts are taken to be within the noise level of the inversion method.

When data corresponding to the most shallow angles of incidence (about 36 degrees or a ray parameter of 11 sec/deg) were left out of the inversion, results were considerably poorer. Little change takes place in the first three layers of case B, which remain substantially unaltered from case A. Layer four, however, is much more poorly resolved. Somewhat more of the sphere is projected onto this layer. The contrast on this layer is somewhat higher than on layer four of Case A : 2.5 percent, but still substantially lower than on the layers where the sphere is actually located. Layer five now shows some consistent structure but has very low contrast.

When travel time residuals are calculated by the plane wave method, calculated ray parameters and azimuths differ from those of the actual plane wave used to generate the data. These differences are a function of both the shape of the velocity inhomogeneities and the station distribution. Because rays are no longer traced along their correct paths, errors result in the final inversion. The causes of the travel time residuals are assigned to the wrong blocks of the initial

model. Two parameters, namely the plane wave's azimuth and ray parameter must also be determined from the data of each event, thus the degrees of freedom are reduced by two. For this reason residuals tend to be smaller than those computed by the "P.D.E.-J.B." method. As a consequence the inversion of the plane wave data is expected to show less contrast in velocity perturbations, than does its "P.D.E.-J.B." analogue. Examination of Figures 1C and 1D show both of these features. The maximum contrast is lower than in Cases A and B : about 7 percent as compared to 8 percent. Regions of positive velocity perturbation occur outside the region occupied by the sphere, along the edges of the resolved area. Once again the presence of data with large ray parameter greatly increases the depth resolution of the inversion.

Although the considerable success of the inversion method in inverting data for a spherical velocity anomaly imbedded in a homogeneous half space does not guarantee its successful application to inverting Tarbela - or any other - structure, it provides credibility toward the notion that such an inversion can be used to study medium scale geologic structures. Caution must be exercised in assigning minimum depths to the bottom of structures since a ^{significant} downward projection of structures occurs unless events with large ray parameters are used. The problem of downward projection of structures is taken to be of secondary importance in the

Tarbela inversion because the data used in that inversion contains ~~these~~ large ray parameters.

Table One

Synthetic data used in Inversion

<u>ray parameter</u> <u>(sec/deg)</u>	<u>distance to</u> <u>event (deg)</u>	<u>angle of in-</u> <u>cidence (deg)</u>	<u># of</u> <u>events</u>	<u>azimuthal</u> <u>spacing (deg)</u>
3	110	10	25	14.4
7	60	22	50	7.2
11	20	36	20	18.0

Table Two

A. Initial Model used in Inversion

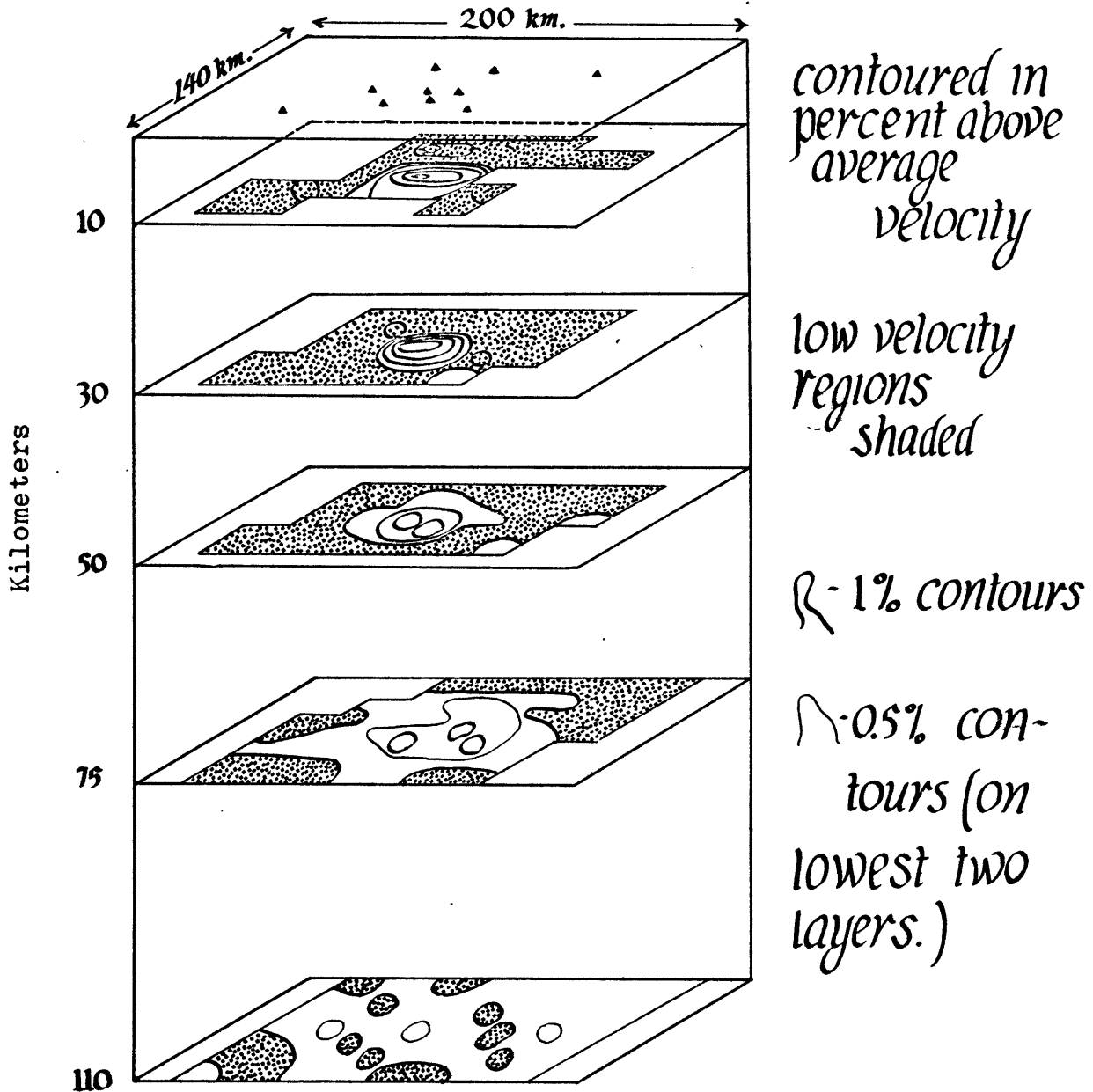
<u>Layer</u>	<u>box size (km)</u>	<u>thickness (km)</u>	<u>initial velocity (km/sec)</u>
1	20 x 20	20	6.0
2	20 x 20	20	6.0
3	20 x 20	20	6.0
4	20 x 20	30	6.0
5	20 x 20	40	6.0

B. Data for individual Inversions

<u>Case</u>	<u>method</u>	<u>ray parameter (sec/deg)</u>	<u>% improvement in account- ing for residuals</u>
A	"PDE-JB"	3,7,11	90
B	"PDE-JB"	3,7	95
C	plane wave	3,7,11	90
D	plane wave	3,7	90

Reconstruction of Sphere in Half Space

Carbela Array Synthetic Data for $p = 3, 7, 11$ sec/deg

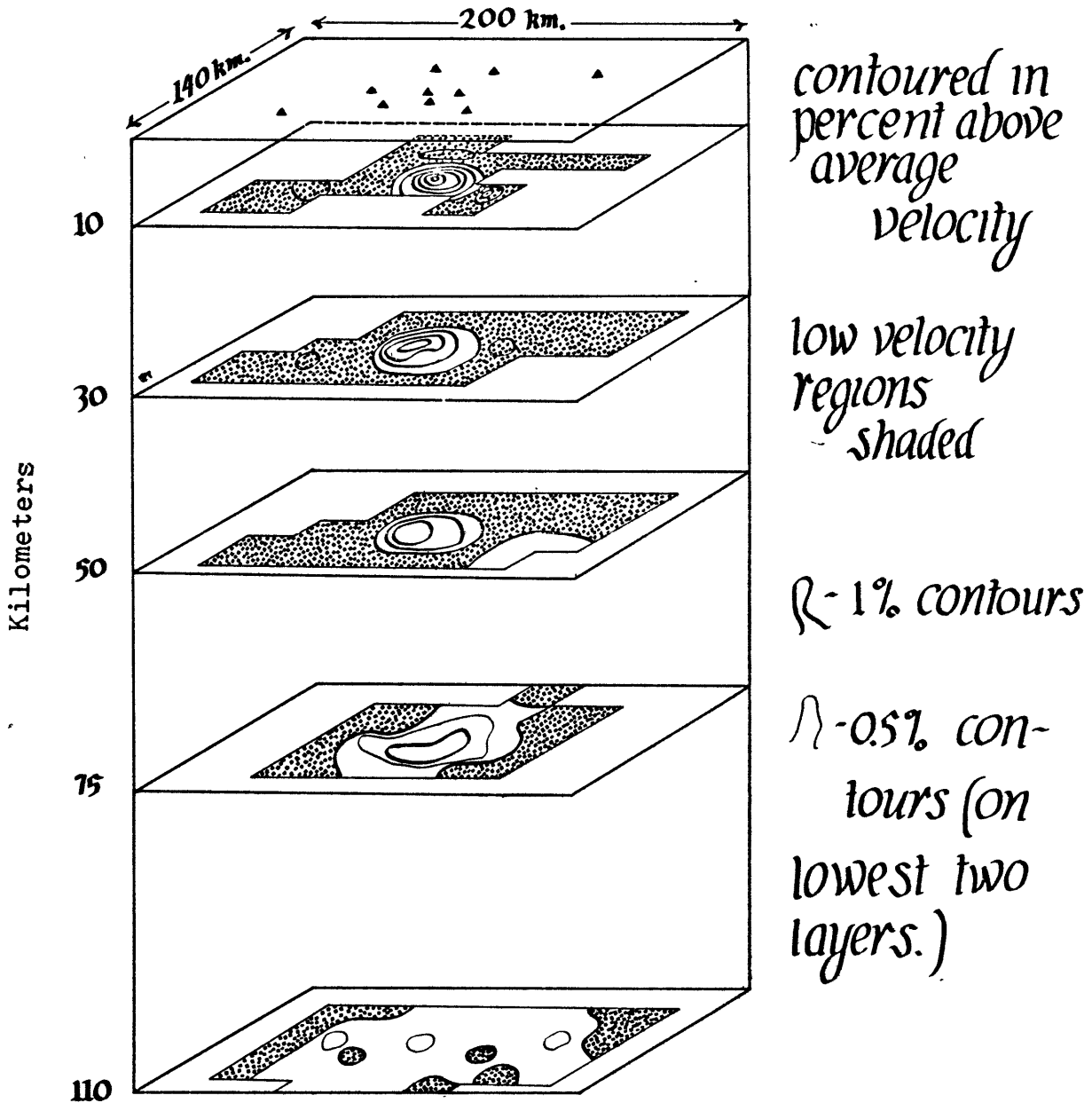


vertical exaggeration 4:1
"p.d.e.-j.b." data

Figure 1A : Synthetic travel time residuals corresponding to a spherical velocity anomaly imbedded in a homogeneous half space are inverted for both data processing methods and two choices of data coverage. In the most accurate inversion of the four shown the inversion (continued on next page)

Reconstruction of Sphere in Half Space

Carbela Array Synthetic Data for $p = 3, 7 \text{ sec/deg}$

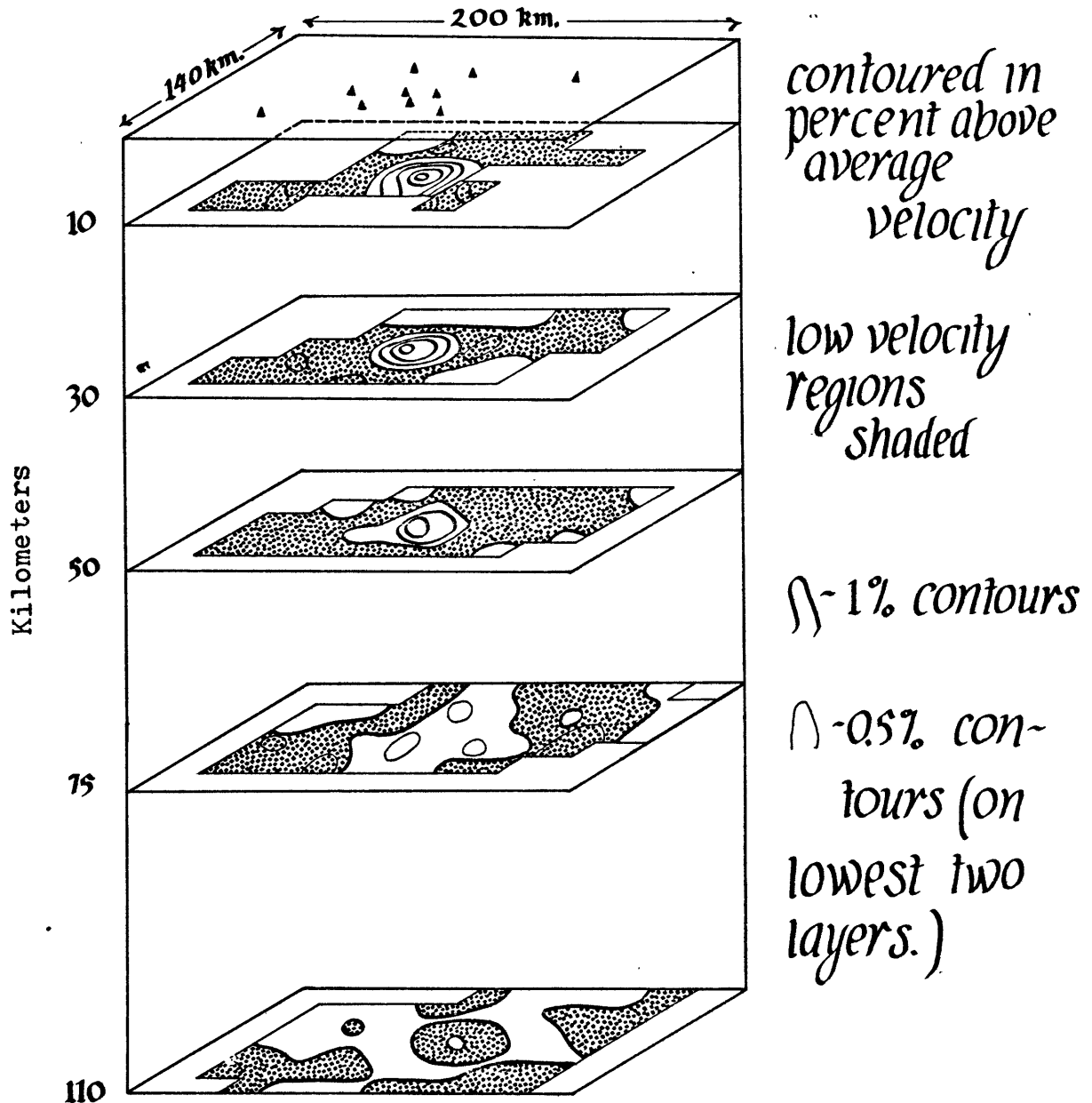


vertical exaggeration 4:1
"p.d.e.-j.b." data

Figure 1B : shows the sphere extending to layer four, whereas it really ends in layer three at a depth of 55 kilometers. This exemplifies the major deficiency of the inversion scheme : its tendency to vertically smooth structures.

Reconstruction of Sphere in Half Space

Arbela Array Synthetic Data for $p = 3, 7, 11 \text{ sec/deg}$

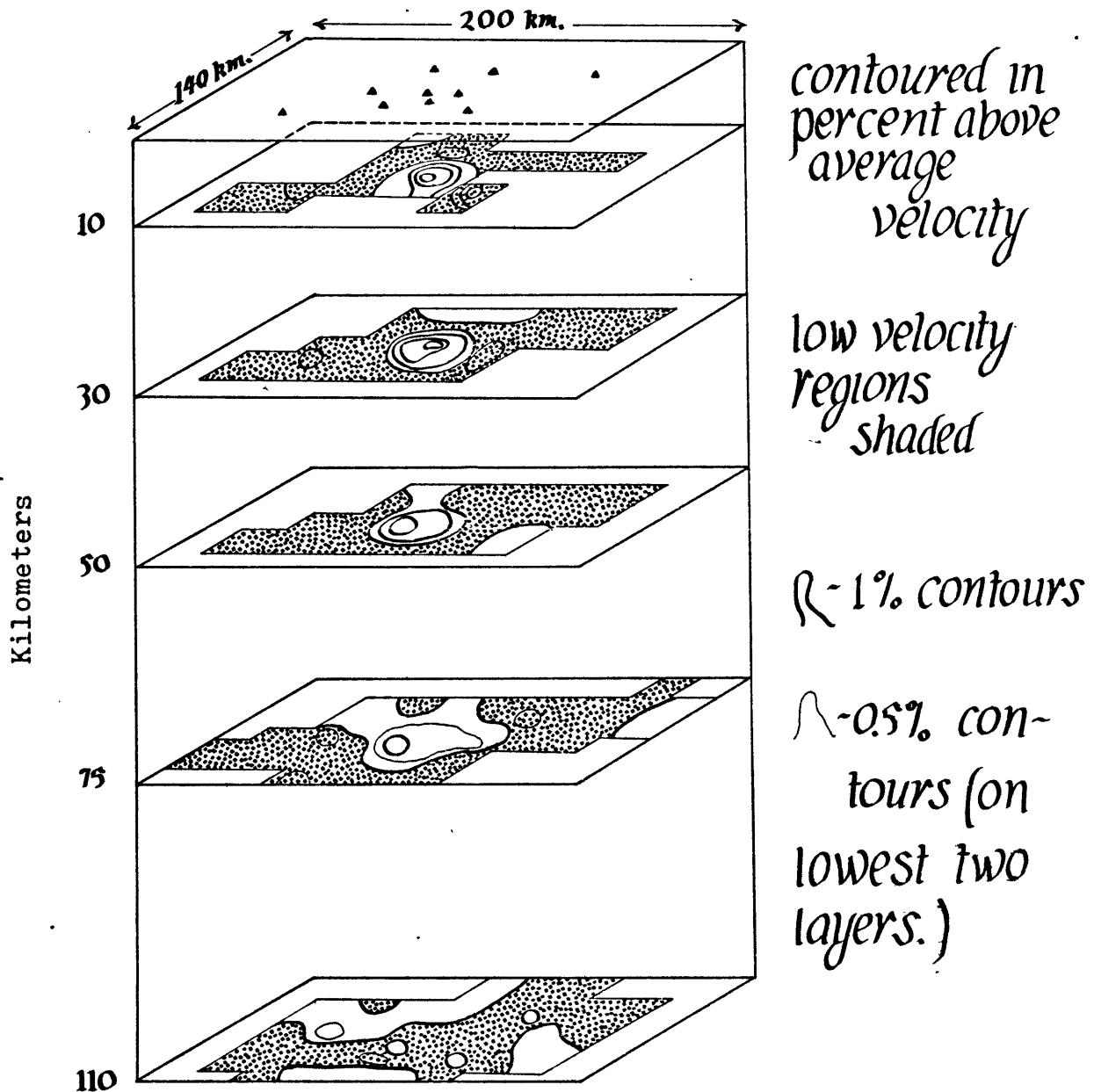


vertical exaggeration 4:1
plane wave data

Figure 1C .

Reconstruction of Sphere in Half Space

Carbela Array Synthetic Data for $p = 3, 7 \text{ sec/deg}$



vertical exaggeration 4:1
plane wave data

Figure 1D .

Acknowledgements

Advice and encouragement from many persons greatly facilitated the conducting of this research. Among these persons I would particularly like to recognize and thank:

Peter Molnar, my advisor (M.I.T.), for many hours of discussion and advice and for financial assistance ;

Klaus Jacob (Columbia University) for providing access to Tarbela Array records ;

Michael Fehler (M.I.T.), William Ellsworth (M.I.T.) and Bernard Minster (Cal-Tech) for other helpful suggestions.

Bibliography

Aki, K., A. Christofferson and E.S. Husebye, Determination of the Three Dimensional Seismic Structure of the Lithosphere, J. Geophy. Res. , in press 1976

Calkins, J., et al, Geology of the South Himalaya in Hazara, Pakistan and adjacent areas, Geologic Survey Paper 716-c, 1972

Chakravorty, K.C. and Ghosh, D.P., Seismological Study of Crustal Layers in Indian Region from the Data of Near Earthquakes, Proc. World Conference on Earthquake Engineering, Tokyo, 1633-1643, 1960

Chouhan, R.K.S. and Singh, R.N., Crustal Studies in Himalayan Region, J. Indian Geoph. Un., 2(1), 51-57 1965

Davies, D. and Sheppard, R.M., Lateral Heterogeneties in the Earth's Mantle, Nature, Vol. 239, No. 5371 pp 218-323, 1972

Kaila, K.L., Reddy, P.R. and Narain, H., Crustal Structure in the Himalayan Foothills Area of North India, From P wave data of shallow earthquakes, Bull. Seis. Soc. Am. 58(2) pp 597-612

LeFort, P., Himalayas: The Collided Range. Present Knowledge of the Continental Arc, Amer. J. Sci. , 275-A, 1975

Levenberg, K., A Method for the Solution of certain Non-linear Problems in Least Squares., Quart. Appl. Math. , 2, pp 164-168, 1944

Menke, William and Jacob, Klaus, Seismicity Patterns in Pakistan and Northwestern India - a comparison of Tarbela Array and WWSSN data, J. Geoph. Res. in press 1976

Molnar, Peter and Tapponnier, Paul, Cenozoic Tectonics of Asia: Effects of a Continental Collision, Science, Vol. 189, No. 4201 pp 419-426 , 1975

Tandon, A.N., and Dube, R.K., 1973, A Study of Crustal Structure beneath the Himalayas from Body Waves, PAGEOPH, III, 2207-2215, 1973

Verma, G.S., Structure of the Foothills of the Himalayas, PAGEOPH, 112, 18-26, 1974

Warsi, Warris E.K., Plate Tectonics and the Himalayan Orogeny, a Modelling Study Based on Gravity Data, Unpublished Master's Thesis, Massachusetts Institute of Technology, 1976